

See discussions, stats, and author profiles for this publication at: <https://www.researchgate.net/publication/51199536>

# Catalytic Steam Gasification of Biomass: Catalysts, Thermodynamics and Kinetics

ARTICLE *in* CHEMICAL REVIEWS · JUNE 2011

Impact Factor: 46.57 · DOI: 10.1021/cr200024w · Source: PubMed

---

CITATIONS

79

READS

115

## 4 AUTHORS, INCLUDING:



[H. De Lasa](#)

The University of Western Ontario

240 PUBLICATIONS 3,427 CITATIONS

[SEE PROFILE](#)



[Jahirul Mazumder](#)

The University of Western Ontario

10 PUBLICATIONS 112 CITATIONS

[SEE PROFILE](#)

## Catalytic Steam Gasification of Biomass: Catalysts, Thermodynamics and Kinetics

Hugo de Lasa,\* Enrique Salaices, Jahirul Mazumder, and Rahima Lucky

Chemical Reactor Engineering Centre, The University of Western Ontario, London, Ontario, Canada N6A5B8

### CONTENTS

1. Introduction	5404	5.1. Kinetic Modeling	5426
2. Steam Gasification of Biomass	5406	5.2. Time Scale Analysis	5426
2.1. Types of Biomass	5406	5.3. Kinetic Models at Particle Scale	5427
2.2. Chemical Characteristic of Plant Biomass	5408	5.4. Intrinsic Kinetics for Biomass Gasification: The CREC "Additive Effect" Model	5427
2.3. Physical Characteristic of Plant Biomass	5410	6. Conclusions and Future Prospects	5428
2.3.1. Biomass Size	5410	Author Information	5429
2.3.2. Biomass Structure	5411	Biographies	5429
2.4. Chemistry of Gasification	5411	Acknowledgment	5430
2.5. Design of Gasifiers	5412	Notation	5430
2.5.1. Fixed-Bed Gasifiers	5412	Greek Symbols	5430
2.5.2. Fluidized-Bed Gasifiers	5413	Acronyms	5430
2.5.3. Advantages/Disadvantages of the Different Gasifying Reactors	5414	References	5430
2.6. Gasifier Operating Conditions	5414		
2.6.1. Equivalence Ratio	5414		
2.6.2. Operating Temperature	5415	1. INTRODUCTION	
2.6.3. Operating Pressure	5415		
2.6.4. Gasifying Agents	5415	Biomass, a hydrocarbon material mainly consisting of carbon,	
2.6.5. Residence Time	5415	hydrogen, oxygen, nitrogen, and minerals, is considered an ideal	
2.7. Advantages and Technical Challenges for Biomass Gasifiers	5415	renewable resource given its abundance, its lower sulfur content,	
3. Catalysts for Steam Gasification of Biomass	5415	and its CO <sub>2</sub> -neutral emissions. In catalytic biomass gasification,	
3.1. Dolomite, Olivine, and Alkali Metal-Based Catalysts	5415	zero net emissions of carbon dioxide can be achieved because	
3.2. Nickel-Based Catalysts	5417	the carbon dioxide released from biomass is quantitatively	
3.2.1. Catalyst Deactivation	5418	recycled back into plants via photosynthesis. <sup>1</sup> Biomass gasifica-	
3.2.2. Effect of Catalyst Support and Dopants	5418	tion produces very low levels of particulates, as well as very little	
4. Thermodynamics of Steam Gasification of Biomass	5419	amounts of NO <sub>x</sub> and SO <sub>x</sub> when compared with fossil fuels. <sup>2</sup>	
4.1. Nonstoichiometric Approach	5419	Moreover, biomass can be used as a source to produce various	
4.2. Thermodynamic Modeling of Biomass Gasification	5419	chemical species. <sup>3</sup>	
4.3. CREC Thermodynamic Biomass Gasification Model	5420	Biomass from plants was the first fuel used by humans to meet	
4.3.1. Equilibrium Constants	5421	their energy demands. In the 19th century, the discovery of fossil	
4.3.2. Distribution of Product Species	5421	fuels helped to industrialize the world and improve standards of	
4.4. Thermodynamic Analysis of Coke Formation	5423	living. It displaced, however, quite considerably the use of	
4.5. Gas-Phase Reactions: At Thermodynamic Equilibrium or Kinetically Limited?	5424	biomass as a fuel. In addition, the production and consumption	
4.6. Optimizing Gasifier Operating	5425	of fossil fuels have caused environmental damage by increasing	
5. Kinetic Studies of Catalytic Steam Gasification of Biomass	5426	the CO <sub>2</sub> concentration in the atmosphere. <sup>4</sup> As the world's	
		accessible oil reservoirs are gradually depleted, it is important	
		to develop suitable long-term strategies based on the utilization	
		of renewable fuel that will gradually substitute the declining fossil	
		fuel production.	
		In this respect, plant biomass is the only currently sustainable	
		source of organic carbon and biofuels. <sup>5</sup> The 220 billion dry tons	
		of annual available biomass (ca. 4500 EJ of energy content)	
		potentially represents the world's largest sustainable energy	
		source. <sup>6</sup> As a result, it is becoming one of the most important	
		renewable energy sources in our planet's immediate future.	

Received: January 12, 2011

Published: June 08, 2011

Biochemical and thermochemical biomass conversion processes are utilized to produce heat and electricity, as well as various chemical feedstocks. The thermochemical processes that have been studied to date are combustion, pyrolysis, and gasification. Among them, gasification of biomass is one of the most economical and efficient technologies for biomass conversion to energy and an attractive alternative for the thermal conversion of solid waste.

Gasification technology, primarily wood gasifiers, was used to power cars in the early 1920s in Sweden, as a result of the general lack of indigenous petroleum resources and the abundance of biomass resources in the form of wood. Extensive studies were undertaken during the 1939–1945 period to further refine the design of the wood gasifiers, gas cleaning, cooling systems, and gas turbines to optimize their performance on wood waste.<sup>7</sup>

In the 1970s and 1980s, about 40 worldwide companies offered to build biomass gasification plants to produce heat and electricity.<sup>5</sup> Nowadays, the flexibility of gasification technology, combined with the various uses of syngas, allows biomass gasification to be integrated with several industrial processes, as well as with power generation systems.<sup>2,5</sup> The chemical efficiency of gasification exceeds 70%. This allows overall electrical efficiencies of over 40%, using high-pressure gasification coupled with fuel cell generation. Moreover, the use of waste–biomass energy production systems in rural communities is very appealing.<sup>8</sup>

In recent years, biomass steam gasification has become an area of growing interest because it produces a synthesis gas with relatively higher hydrogen content. This syngas could be used for industrial applications, both for highly efficient electricity production and as a feedstock for chemical synthesis.

Catalytic steam gasification of biomass in fluidized beds is a promising approach given its (i) rapid biomass heating, (ii) effective heat and mass transfer between reacting phases, and (iii) uniform gasifier reaction temperature. Moreover, fluidized beds tolerate wide variations in fuel quality as well as broad particle size distributions.

However, a serious issue for the broad implementation of the biomass gasification technology is the generation of unwanted char and tars. Char or biochar is a solid carbonaceous residue. Tar is a complex mixture of condensable hydrocarbons, which includes single-ring to five-ring aromatic compounds along with other oxygen-containing hydrocarbons species. Additional information about tar is provided in Table 4.

Tar can condense in the gasifier pipe outlets and in particulate filters, which leads to blockages and filter clogging. Tar causes further downstream problems and clogs fuel lines and injectors in internal combustion engines. According to Milne et al.,<sup>9</sup> “tar is the most cumbersome and problematic parameter in any gasification commercialization effort”. For commercial applications, tar components have to be limited to <1 g/m<sup>3</sup> of gas at standard temperature and pressure (STP) conditions. Therefore, considerable efforts are currently underway to find a manner to remove tar from fuel gas.

The different approaches for tar removal to date can be categorized as follows: (i) direct synthesis gas treatment inside the gasifier (primary methods) and (ii) hot gas cleaning after the gasification process (secondary methods). Primary treatment methods are the ones gaining much attention nowadays as they may eliminate the need for additional downstream equipment using hot-gas cleaning technology.

There are several factors to consider toward the development of an effective primary tar treatment method: (a) the proper selection

of operating parameters, (b) the type of additive/catalyst used, and (c) the needed modifications in gasifiers to prevent tar buildup. Tar can be converted thermally. However, this typically requires very high temperatures, >1000 °C. According to Devi et al.,<sup>10</sup> the catalytic reforming of tars into gaseous products is an effective method for tar removal, avoiding costly tar disposal. In this respect, Ni-based catalysts can contribute given their ability to convert tar and their water gas shift activity as well as their capacity in reducing nitrogen-containing compounds such as ammonia.

However, several deactivation mechanisms occur with nickel-based catalysts including poisoning with sulfur, chlorine, and alkali metals, sintering of Ni particles, and coke formation. Under these conditions, Ni-based catalysts deactivate rapidly due to coke.<sup>11</sup> While coke can be removed by combustion, coke removal can lead, if not carefully performed, to poor catalyst activity, selectivity, and limited catalyst life. Coke deposition can also be minimized through the use of excess steam with respect to the one required by gasification stoichiometry.<sup>12</sup> In practice, this increases the overall energy costs for gasification plant operation.

Furthermore, there is a remaining solid inorganic residue left after gasification that is designated as ash. It is highly desirable to keep the operating temperature of the gasifier below 700 °C, to prevent ash agglomeration. Ash frequently contains CaO, K<sub>2</sub>O, P<sub>2</sub>O<sub>5</sub>, MgO, SiO<sub>2</sub>, SO<sub>3</sub>, and Na<sub>2</sub>O that can sinter, agglomerate, and deposit on surfaces and contribute to erosion and corrosion of the gasifier.<sup>13</sup> Furthermore, alkaline metals react readily in the gasifier with silica-forming silicates or with sulfur-producing alkali sulfates, leaving a sticky deposit and in many instances causing bed sintering and defluidization.<sup>14–16</sup>

Synthesis gas, produced from biomass, is required to be cleaned from trace amounts of H<sub>2</sub>S, COS, CS<sub>2</sub>, HCl, NH<sub>3</sub>, and HCN at the ppb level. To accomplish this without a negative impact on process thermal efficiency, the synthesis gas has to be cleaned at high temperatures.<sup>17</sup> In this regard, Leibold et al.<sup>18</sup> has considered a high temperature–high pressure cleaning process with the syngas produced being suitable for Fischer–Tropsch synthesis.

Catalytic biomass gasification is a complex reaction process that includes numerous chemical reactions such as pyrolysis, steam gasification, and water gas shift reaction.<sup>19</sup> Extensive research has been made to develop stable and highly active catalysts for biomass gasification producing high-quality synthesis gas and/or hydrogen.<sup>10,20–26</sup> However, designing an optimum catalyst for steam gasification requires additional insights into gasification kinetics and reaction mechanisms to predict the end-reaction product composition distribution. Furthermore, long-life catalysts for biomass steam gasification are required for large-scale processes to operate in the 700–800 °C range, yielding H<sub>2</sub>/CO ratios of ~1 or even higher, suitable for the alternative manufacturing of fuels such as ethanol and biodiesel.<sup>27</sup>

To date, a significant volume of research on thermodynamic models provides valuable tools to predict an approximate product composition under various gasification operating conditions. Although these models provide satisfactory predictions of the H<sub>2</sub>/CO ratio, in most cases the observed synthesis gas compositions deviate from chemical equilibrium predictions.<sup>19</sup> Specifically, experimental methane composition, a very critical parameter that is used to define the heating value of the synthesis gas, deviates considerably from most of the model-predicted thermodynamic values. The main reasons for this deviation are due to some inadequate assumptions adopted such as the following: (i) assumed equilibrium conditions for some key

reaction steps, (ii) char and tar accumulation being considered as solid carbon, and (iii) ash being treated as an inert species. It is well acknowledged that, in an actual process, various gasification reactions cannot reach chemical equilibrium and that the above-mentioned deviations are affected by the different reactivities of char/tar. Furthermore, even the ash can have positive catalytic activity in the pyrolysis step, which may influence the synthesis gas composition.

Therefore, reactor design and operation call for suitable phenomenologically based reaction kinetics adaptable to various biomass feedstocks and suitable for unit scale-up. It is our view that a critical and up-to-date review of gasification reaction mechanisms and kinetics, as is provided in this paper, gives valuable information and future direction for reaction engineering and process design in the context of biomass catalytic gasification.

Several books, book chapters, and a significant volume of review articles have been published in the technical literature focusing on different issues such as (i) tar removal, (ii) catalyst for biomass gasification, (iii) hot gas cleaning, and (iv) characteristics of biomass. These are all important factors in biomass gasification technology.

However, and in spite of the significance of all this, there is no comprehensive review on biomass catalytic gasification with emphasis on thermodynamics, kinetics, and catalyst properties as well as feedstock characteristics. We believe that, in all these respects, this is a timely contribution. We anticipate that this review will promote research and development efforts, scale-up of the gasification process, and large-scale implementation of catalytic steam gasification of biomass.

In this article, research contributions are reported according to the following sections:

- In section 2, we review the steam gasification process with main emphasis given to the chemical and physical characteristic of plant biomass, gasifier designs, and operating conditions. This is done to provide a general background and allow the reader to understand the influence of operating variables on biomass gasification.
- In section 3, we give an account of catalysts used for steam gasification. Main emphasis is given to the nickel catalyst and to the new catalytic materials being investigated by CREC-UWO researchers.
- In section 4, we discuss thermodynamics studies of steam gasification of biomass, and particularly we describe a new thermodynamic model recently formulated by the CREC-UWO research team. Emphasis is placed on the general applicability of this thermodynamic equilibrium model to different biomass feedstocks and for reaction times larger than 20 s.
- In section 5, we review biomass gasification reaction engineering. We also elaborate on the very important advances of the CREC-UWO researchers on kinetic modeling using an “algebraic addition” of reaction rates of the main catalytic reactions contributing to biomass gasification.
- In section 6, we provide concluding remarks and future prospects for catalytic gasification technology.

## 2. STEAM GASIFICATION OF BIOMASS

There are different biomass conversion processes utilized to produce heat and electricity, as well as to convert biomass into various chemical species. Thermochemical transformation or gasification of cellulose or lignocellulose into synthesis gas

(CO + H<sub>2</sub>) is possible above 700 °C in the presence of controlled amounts of oxygen. On the other hand, if lignocelluloses are heated in the absence of oxygen, then a mixture of gases, bio-oils, tars, and char are generated. This pyrolysis process requires a high energy input.

There is another method for the conversion of cellulose using hot and compressed sub- and/or supercritical water. Supercritical water gasification of biomass is a technology especially recommended for wet biomass where no biomass drying is required.<sup>28,29</sup> In addition to the interesting prospects of forming less tar and char, supercritical water gasification can produce a significant fraction of extra hydrogen originating in the water rather than in the biomass.<sup>30,31</sup> Supercritical water displays high acidity, and thus, the reactor materials are prone to corrode. As a result, the process is penalized for its high capital costs, requiring a large monetary investment.

The hydrolysis of cellulose with mineral acids or enzymes has been used for a quite a number of years already. However, its commercial use is hindered by problems associated by the following: (i) degradation of monomers, (ii) corrosion risk, (iii) handling and storage of acids/enzymes, (iv) generation of neutralized waste, and (v) separation of the product.<sup>14,32</sup>

In recent years, steam biomass gasification has become an area of growing interest because it produces a gaseous fuel with relatively high hydrogen content. Synthesis gas can be used for industrial applications, including efficient electricity production, and as a feedstock for chemical synthesis.

Theoretically, almost all kinds of biomass with moisture content in the 5–30 wt % range can be gasified. However, it is known that feedstock (biomass) properties, such as (i) specific surface area, (ii) size, (iii) shape, (iv) moisture content, (v) volatile matter, and (vi) carbon content, all affect gasification. Other variables that also significantly influence gasification are (a) the gasifier configuration, (b) the specific gasification process conditions used, and (c) the gasifying agent.

A detailed review of the many biomass conversion processes shows that no individual process is without drawbacks.<sup>33</sup> Thus, it is critical to find an effective and efficient biomass conversion technology to utilize this renewable energy resource. It is in this respect essential to understand the gasification chemistry to determine the influence of each variable on gasification. Furthermore, one must also study the full feedstock to establish both the contribution by the individual lump components and the possible interactive effects of various biomass constituents.

In the following section, the several variables affecting the gasification process, such as (i) chemical and physical biomass characteristics, (ii) operating conditions, and (iii) gasifier design, are reviewed.

### 2.1. Types of Biomass

Biomass is organic matter derived from plants and waste. Researchers characterize the various types of biomass by dividing them into four major categories:<sup>3</sup>

- (i) *Energy crops.* Energy crops are those grown especially for the purpose of producing energy encompassing short-rotation or energy plantations: they comprise herbaceous energy crops, woody energy crops, industrial crops, agricultural crops, and aquatic crops. Typical examples are eucalyptus, willows, poplars, assorghum, sugar cane, artichokes, soya beans, sunflowers, cotton, and rapeseed such as *Salix Viminalis*, *Miscanthus X Giganteus* (MXG), and *Andropogon Gerardi*. Energy crops are suitable to be used

in combustion, pyrolysis, and gasification for the production of biofuels, synthesis gas, and hydrogen.<sup>34</sup>

**Table 1. Ultimate Analyses of a Diverse Variety of Biomass Compositions**

biomass	ultimate analysis					$C_xH_yO_z$			
	C	H	O	N	S	x	y	z	ref
jute stick	47.18	8.36	44.10	0.36		1.0	2.11	0.70	46
glucose						1.0	2.00	1.00	
heterotrophic	76.22	11.61	11.24	0.93		1.0	1.81	0.11	46
potato starch	42.50	6.40	50.80	0.00	0.000	1.0	1.79	0.90	47
poplar wood sawdust	42.70	6.20	50.90	0.10	0.100	1.0	1.73	0.89	47
pine sawdust	50.26	6.72	42.66	0.16	0.200	1.0	1.59	0.64	48
legume straw	43.30	5.62	50.35	0.61	0.120	1.0	1.55	0.87	48
rice straw	36.90	4.70	32.50	0.30	0.060	1.0	1.52	0.66	49
softwood bark	77.56	8.69	13.30	0.59		1.0	1.34	0.13	46
pine	51.60	4.90	42.60	0.90		1.0	1.13	0.62	50
waste wood	55.11	6.01	37.99	0.86	0.030	1.0	1.30	0.52	51
coal	75.80	4.40	16.70	1.89	1.220	1.0	0.69	0.17	52

(ii) *Agricultural residues and waste.* Large quantities of agricultural plant residues are produced annually worldwide and are vastly underutilized. The most common agricultural residue is the rice husk, which makes up 25% of rice by mass. Other plant residues include sugar cane fiber (bagasse), coconut husks and shells, groundnut (peanut) shells, and straw. Included in agricultural residue is waste, such as animal manure (e.g., from cattle, chicken, and pigs). Because of the low heating value of the syngas produced using animal manure, manure is not technically feasible as the only gasifier fuel and other potential options have to be considered. For instance, cow dung can be used as a supplementary fuel blended with a conventional woody biomass, like sawdust.<sup>35</sup> Another type of waste from domestic or industrial sources is refuse-derived fuel (RDF). This is a combustible material consisting mainly of plant matter but may also include some waste plastics from garbage. RDF may be used in the raw and untreated variety, in the partially processed form, or in the fully processed form of pellets.

(iii) *Forestry waste and residues.* These wastes and residues include mill wood waste, logging residue, and tree and

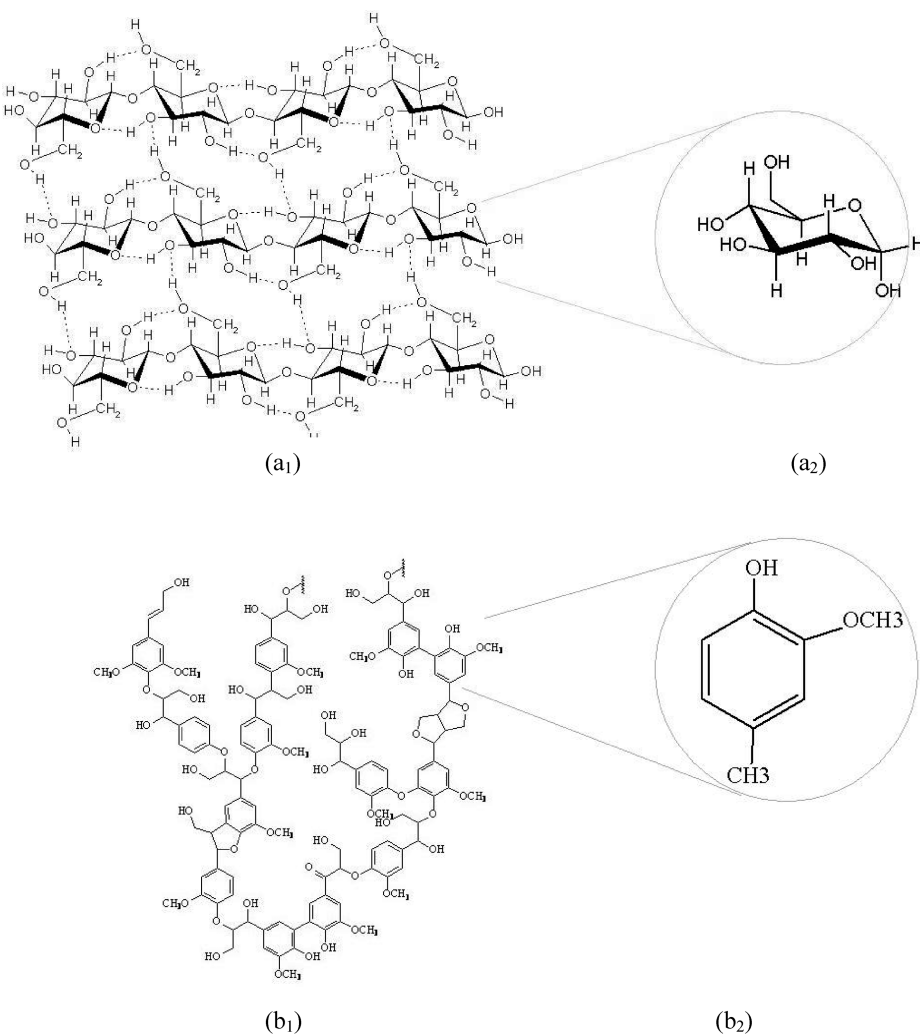


**Figure 1.** (a<sub>1</sub>) Chemical linkages in a cellulose polymer, (a<sub>2</sub>) cellulose surrogate model (glucose) used in gasification experiments; (b<sub>1</sub>) chemical linkages in a lignin polymer, (b<sub>2</sub>) lignin surrogate model (2-methoxy-4-methyl phenol) used in gasification experiments. Adapted with permission from data reported by Salaices in ref 27.

shrub residues. Fuels from wood (wood fuel and charcoal) are derived from natural forests, natural woodlands, and forestry plantations. Wood fuel is the principal source for small-scale industrial energy in the rural areas of developing countries. However, reforestation will be required to meet future energy demands as the world population grows. A possible predominant biomass-derived fuel is from wood-processing industries. The utilization of this residue for energy production at or near its source has the advantage of avoiding expensive transporting costs. Domestic wood fuels are sourced principally from land clearing and logging residues.

- (iv) *Industrial and municipal wastes.* This waste encompasses municipal solid waste (MSW), sewage sludge, and industry waste.<sup>36</sup> Municipal solid wastes and industrial residues such as black liquor from wood pulping also represent potential biomass feedstocks.<sup>37</sup> They pose, however, major problems in gasification technology. Straw and municipal solid wastes may form large amounts of ash deposits in the furnace or convective sections of utility boilers.<sup>38</sup> In this respect, cost-effective methods for the management of remaining ash are actively being studied.<sup>39</sup>

A significant volume of published articles on gasification using various sources of biomass confirmed that thermal degradation kinetics, reactivity, and product characteristics all change with the type of biomass used.<sup>40</sup> The amount and type of char and tar from gasification appear to be composed of different chemical species. These chemical species are a function of the feedstock used and of the different cracking pathways.<sup>41</sup> For example, Kosstrin<sup>42</sup> proved through experiments that the highest yield of tar was 35% for wood, ~60% for paper, and only 30% for sawdust.<sup>43</sup> This was attributed to the fact that gasification products are affected by

biomass chemical composition, as well as moisture content and type of alkali content.<sup>44</sup>

## 2.2. Chemical Characteristic of Plant Biomass

Every biomass type has carbon, hydrogen, and oxygen as major chemical constitutive elements. These element fractions can be quantified with the ultimate analysis. The ultimate analyses of 13 biomass feedstocks are reported in Table 1. Ultimate analyses are reported using the  $C_xH_yO_z$  formula where  $x$ ,  $y$ , and  $z$  represent the elemental fractions of C, H, and O, respectively. On this basis, it can be predicted that given biomass low hydrogen and high oxygen contents, all biomasses have a low calorific value, which is a main disadvantage for direct biomass utilization as an energy source.<sup>45</sup> One can also establish that the oxygen available in biomass only allows 65–87 wt % of the carbon to be converted into CO, while the remaining 13–35 wt % of the carbon requires additional oxygen supply.

Moreover, the products of biomass gasification also depend on the various amounts of inorganic materials that yield ash during the gasification. The ash formed has a significant influence on the gasification itself.<sup>53</sup>

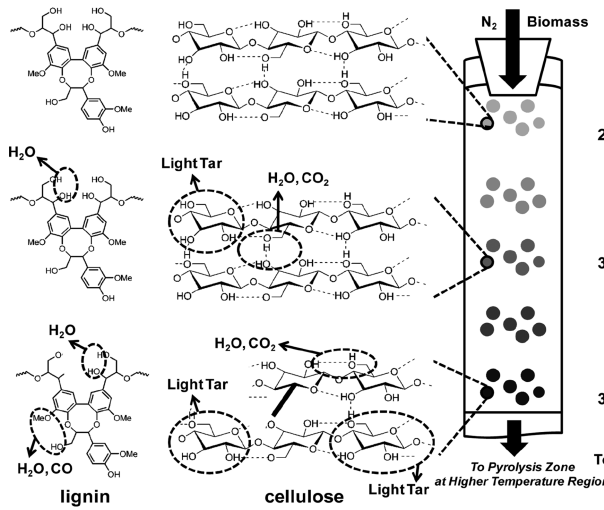
To fully describe biomass characteristics, it is customary to provide, in addition to the ultimate analysis (percentage of carbon, hydrogen, and oxygen), the proximate analysis. This analysis includes the content of moisture, volatile matter, fixed carbon, and ash.

Woody plant species are typically characterized by slow growth and are composed of tightly bound fibers, giving a hard external surface, whereas herbaceous plants are usually perennial, with more loosely bound fibers, indicating a lower proportion of lignin, which binds together the cellulosic fibers. Biomass is mainly formed of hemicellulose, cellulose, lignin, and ash (Table 2). The relative proportions of cellulose and lignin are two of the determining factors in identifying the suitability of plant species for subsequent processing as energy crops.

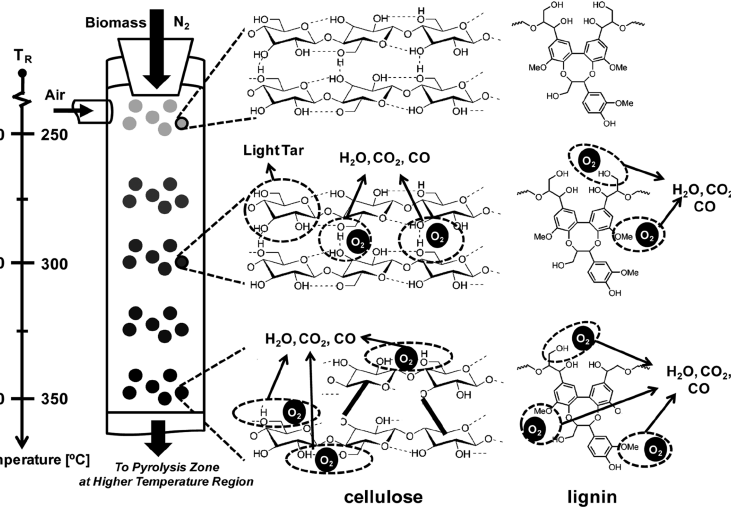
Cellulose is a glucose polymer, consisting of linear chains of glucopyranose units, with an average molecular weight of around 100 000 kg/kmol. Hemicellulose is a mixture of polysaccharides, composed almost entirely of sugars such as glucose, mannose, xylose, and arabinose with an average molecular weight of 30 000 kg/kmol. In contrast to cellulose, hemicellulose is a heterogeneous branched

**Table 2. Typical Compositions of Biomass<sup>1</sup>**

ASTM	E-1821-96	E-1821-96	E-1721-95	E-1755-95
biomass	cellulose (wt %)	hemicellulose (wt %)	Lignin (wt %)	ash (wt %)
hardwood	36.4–50.3	12.7–23.2	16.6–28.6	0.4–9.7



**(a) Nitrogen Treatment**



**(b) Air Treatment**

**Figure 2.** (a) Pyrolysis of biomass in a nitrogen atmosphere and (b) biomass conversion in an air atmosphere.<sup>56</sup>

**Table 3.** Tar Maturation Scheme<sup>5</sup>

	400 °C	500 °C	600 °C	700 °C	800 °C	900 °C
species	mixed oxygenates	phenolic ethers	alkyl phenols	heterocyclic ethers	polynuclear aromatic hydrocarbons	larger polynuclear aromatics

**Table 4.** Chemical Components in Biomass Tars<sup>5</sup>

conventional flash pyrolysis (450–500 °C)	high-temperature flash pyrolysis (600–650 °C)	conventional steam gasification (700–800 °C)	high-temperature steam gasification (900–1000 °C)
acids	benzenes	naphthalenes	naphthalene
aldehydes	phenols	acenaphthylenes	acenaphthylene
ketones	catechols	fluorenes	phenanthrene
furans	naphthalenes	phenanthrenes	fluoranthene
alcohols	biphenyls	benzaldehydes	pyrene
complex	phenanthrenes	phenols	acephenanthrylene
oxygenates	benzofurans	naphthofurans	benzanthracenes
phenols	benzaldehydes	benzanthracenes	benzopyrenes
guaiacols			polyaromatic hydrocarbons
syringols			
complex phenols			

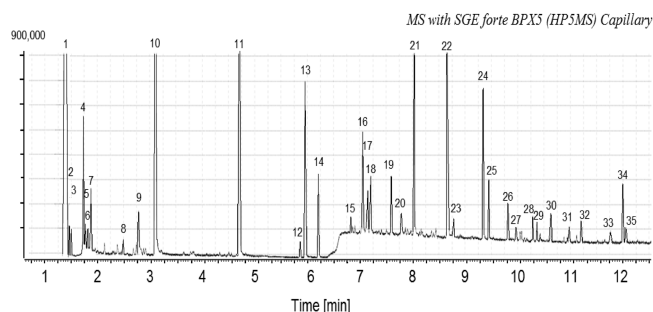


**Figure 3.** Composition of hydrocarbon products from steam gasification of biomass surrogate (2-methoxy-4-methylphenol) at 700 °C, with an S/B ratio of 0.4 and 30 s of contact time.<sup>27</sup> Codes in the chart: 1, methane; 2, ethylene; 3, ethane; 4, 1,3-pentadiene; 5, 2-butene, 2-methyl; 6, 1,3-pentadiene; 7, 1,3-cyclopentadiene; 8, 1,3-butadiene, 2, 3-dimethyl; 9, 1,3-cyclopentadiene; 10, benzene; 11, toluene; 12, ethylbenzene; 13, *o*-xylene; 14, *p*-xylene; 15, benzene, 1-ethyl-3-methyl; 16, phenol; 17, benzene, 1-ethenyl-2-methyl; 18, benzocyclobutene-1(2H)-one; 19, indene; 20, phenol, 3-methyl; 21, 2-propenal, 3-phenyl; 22, naphthalene; 23, phenol, 2-ethyl-5-methyl; 24, naphthalene, 2-methyl; 25, naphthalene, 1-methyl; 26, naphthalene, 1,7-dimethyl; 27, naphthalene, 2,3-dimethyl; 28, 1,1'-biphenyl, 3-methyl; 29, 1-naphthalenol; 30, 2-naphthalenol; 31, 7-methyl-1-naphthol; 32, 9H-fluoren-9-ol; 33, naphtho[2,1-*b*]furan, 1,2-dimethyl; 34, anthracene; 35, phenanthrene.

polysaccharide that binds tightly and noncovalently to the surface of each cellulose microfibril. Lignin can be regarded as a group of amorphous, high molecular weight, chemically related compounds. The building blocks of lignin are believed to be a three carbon chain attached to rings of six carbon atoms, called phenylpropanes. Both woody and herbaceous plant species have specific growing conditions, based on the soil type, moisture, nutrient balances, and sunlight, all of which determine their suitability and productive growth rates in specific geographic locations.<sup>54</sup>

Biomass hemicellulose, cellulose, and lignin constituents decompose in the temperature ranges of 225–325, 305–375, and 250–500 °C, respectively.<sup>55</sup> A schematic representation of

the biomass pyrolysis under inert gas atmosphere and biomass air atmosphere is reported in Figure 2.<sup>56</sup>

Elliott<sup>57</sup> reviewed the composition of biomass pyrolysis products and gasifier tars from various processes. Tables 3 and 4 show the expected transition from primary products to phenolic compounds to aromatic hydrocarbons, as a function of process temperature.

Furthermore, Figure 3 reports the composition of products derived from atmospheric-pressure gasification of biomass at 700 °C, with an S/B ratio of 0.4 and with 30 s contact time in a CREC riser simulator. A biomass surrogate (2-methoxy-4-methylphenol) is used in this process. The figure shows the aromatics and oxygenate species fractions contained in the tar ( $C_6^+$ ) fraction.<sup>27</sup>

The variation of constituent fractions in biomass gives products with a different heating value. Furthermore, and taking into account that lignin gasification produces more hydrogen than other components of the biomass, pretreatments that improve lignin content are important.<sup>58</sup> Regarding biomass constituents, there is still controversy regarding the possible interactions among the different components of biomass during gasification.<sup>43,53,59–61</sup>

It was observed in this respect that the formation of water-soluble tars occurs mainly in the early stages of pure cellulose gasification. This is in contrast with the lower water-soluble tar yields obtained with full biomass. In this respect, significant interactions such as cellulose–lignin were observed in pyrolysis. It appears that lignin inhibits the thermal polymerization of levoglucosan as well as enhances the formation of low molecular weight products from cellulose. This, in turn, reduces the yields of char and the secondary char formation from lignin. As a result, this improves the production of some lignin-derived species such as guaiacol, 4-methylguaiacol, and 4-vinylguaiacol. Comparatively weak interactions were also observed in cellulose–hemicellulose pyrolysis.<sup>62</sup>

Furthermore, the yields of water-insoluble tars formed from pure cellulose are substantially less than from full biomass. This shows that there are interactions between lignin, cellulose, and hemicellulose biomass components during gasification.

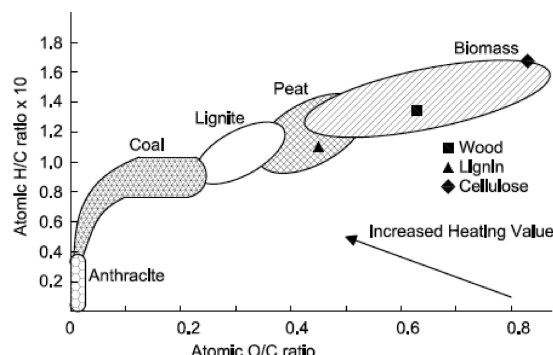


**Figure 4.** Van Krevelen's diagram showing the various H/C ratios and O/C ratios for different feedstocks. Adapted with permission from ref 54. Copyright 2002.

Biomass pyrolysis also yields a solid product residue, the char. T-Raman spectroscopy has been used to analyze the structure of chars and biochars. In the case of biochars, it has been shown that they are highly heterogeneous and disordered structures. Biochar gasification can be significantly influenced by the inherent alkali and alkaline soil metallic contents (AAEM). In fact, the AAEM present in raw biochars can act as a catalyst accelerating some gasification steps.<sup>63</sup> This AAEM effect, however, appears to have little influence on the structural properties of biochars, such as pore surface area.<sup>64</sup>

Mineral matter and mineral concentration are dependent on genotype as well as on the location in which the plants are grown. However, biomass mineral concentration cannot always be easily related to the mineral soil content.<sup>65</sup> While biomass is converted, ash can be traced to the biomass mineral matter content. Ash offers challenges to biomass conversion including sintering, agglomeration, deposition, erosion, and corrosion. These are the main obstacles to economical and viable applications of biomass gasification technologies.<sup>66</sup> Furthermore, it is well documented that ash contributes as a catalyst. Ash may at the same time reduce the H<sub>2</sub> yields in the air gasifier.<sup>50,66,67</sup>

Raveendran et al.<sup>68</sup> have studied the influence of mineral matter in pyrolysis by demineralizing the biomass and then impregnating it with salts. This study has reported the following:

- (1) Demineralized biomass yields higher tar fractions.
- (2) Demineralized biomass increases char yields, as in the case of coir pith, groundnut shell, and rice husk.
- (3) Demineralized corn cob and wood reduces char yields.
- (4) Demineralized rice husk yields higher char yield than coir pith and groundnut shell.

One should notice that, with temperature variations, the amount of ash emissions may also vary. In the 100–500 °C range, a small fraction of the ash may be emitted. Above 600 °C, ash releases can increase sharply. In fluidized bed gasifiers, however, ash emissions may be significantly reduced due to particle–particle collisions and, as a result, enhanced ash agglomeration.

Moreover, ashes, which are continuously produced and normally disposed of in landfills, may have an adverse effect on the environment. Small ash particles may contribute to both air pollution and groundwater pollution through metal leaching.

Ash can be used as a pozzolanic material mixed with concrete or cement. This reduces both the consumption of concrete and cement and landfill area requirements. This in turn can help decrease the environmental impact caused by concrete and cement manufacturing involving both high energy consumption and CO<sub>2</sub> emissions.<sup>69</sup>

Moisture is an important constituent in biomass. Moisture content should be determined on an ash-free basis. Although water is needed for a suitable gasification,<sup>70,71</sup> a moisture content that is too high means that more air for combustion is needed to sustain the gasifier temperature. Although higher gasification temperatures may lead to better carbon conversion and lower tar emissions, these temperatures may also give a synthesis gas with lower heating value and, as a result, lower synthesis gas utilization efficiency.

Biomass gasification can be studied in principle, using as a starting point the components of biomass.<sup>72</sup> There is, however, as stated above, evidence of interactions among the components of the biofeedstock while being gasified. These observations are based on thermogravimetric analysis (TGA) and differential thermogravimetric analysis (DTG) obtained at different heating rates for full biomass, pure wood, pure cellulose, pure hemicellulose, and pure lignin. Thermograms for all these cases display different temperatures at maximum weight losses ( $T_m$ ) as follows:

- (1) For pure hemicellulose, pure cellulose, and pure lignin, single  $T_m$  values were observed.
- (2) For wood, two  $T_m$  values were recorded. These two  $T_m$ 's were close to the ones for pure cellulose and pure hemicellulose.

Gasification of biomass with varying elemental compositions of organic matter can be assessed in a Van Krevelen's diagram<sup>73</sup> in terms of hydrogen/carbon (H/C) and oxygen/carbon (O/C) ratios as described in Figure 4. Wood, cellulose, and lignin are represented in this diagram together with coal and peat. It can be observed, in this respect, that exergy losses in wood gasification (O/C ratio ≈ 0.6) are larger than those for coal (O/C ratio ≈ 0.2). Thus, for a fuel with an O/C ratio below 0.4 and a lower heating value (LHV) of >23 MJ/kg, a gasification temperature of 927 °C is recommended. On the other hand, for a fuel with O/C ratio below 0.3 and a LHV of 26 MJ/kg or more, a 1227 °C gasification temperature is preferred.

As a result of this, it could thus be attractive to modify the properties of oxygenated biofuels prior to gasification as follows: (i) by separation of wood into its components with gasification of the lignin performed at a later process step and (ii) by thermal pretreatment, and/or biomass mixing with coal, to enhance the heating value of the solid fed to the gasifier.<sup>74</sup>

### 2.3. Physical Characteristic of Plant Biomass

Several pretreatments are performed in biomass gasification facilities in an effort to precondition the feedstock such as (i) drying, (ii) size reduction, (iii) size fractionation, and (iv) leaching with water. One should notice, however, that the degree of pretreatment of the biomass feedstock is dependent on both the fuel and the gasification technology used.<sup>75,76</sup>

**2.3.1. Biomass Size.** Since pyrolysis and gasification of biomass are thermochemical processes, the temperature and rates of particle heating have pronounced effects on the weight loss of biomass. To achieve this, the smaller the biomass size, the better is the fluid–particle heat transfer. If the temperature is uniform throughout the particle, this yields a more controlled gasification. Moreover, whenever the intrinsic kinetics controls the overall gasification process, gasification rates increase exponentially with temperature following Arrhenius' rate law.

One has to be aware that, given that biomass particle size reduction is quite an intensive energy process, particle size should not be smaller than required. Maa and Bailie<sup>77</sup> have

shown that, in the pyrolysis of cellulose, the intrinsic reaction rate controls the overall gasification for particles smaller than 0.2 cm. For particles in the 0.2–6 cm size range, both heat transfer and intrinsic reaction rate have an influence on the gasification. For particles larger than 6 cm, the gasification rate becomes fully controlled by heat transfer.<sup>53</sup>

Erlich et al.<sup>78</sup> studied the effects of (i) classification, (ii) source, (iii) size, and (iv) shape of biomass during slow pyrolysis and steam gasification. This research group reported that the biomass pellet size has an impact on the gasification rate but only very slightly on pyrolysis rate. The larger the pellet, the slower the gasification becomes. Moreover, a recent report showed that char combustion reactivity can be increased in larger biomass particles (1.5–5.18 mm), increasing the alkaline metal content species concentration.<sup>79</sup>

**2.3.2. Biomass Structure.** Biomass is frequently a highly porous material with a very high surface area. Diffusion of the reactants and products in many instances takes place under nonrestricted molecular transport. Furthermore, when the biomass is highly porous, uniform temperature can be achieved in biomass pellets resulting in homogeneous gasification in all portions of biomass, yielding uniform composition of product gases. On the other hand, when biomass is less porous, the temperature may vary from a maximum temperature at the pellet exterior to a minimum value at the center. In those cases, gasification on biomass exterior surfaces may dominate, with biomass external surface shrinking throughout the gasification. Because of the nonuniformity of temperature, drying, pyrolysis, and gasification, these processes may take place concurrently, yielding nonuniform composition of gases.<sup>53</sup>

#### 2.4. Chemistry of Gasification

Gasification is a thermochemical conversion process of solid biomass into a gas-phase mixture of carbon monoxide (CO), hydrogen (H<sub>2</sub>), carbon dioxide (CO<sub>2</sub>), methane (CH<sub>4</sub>), organic vapors, tars (benzene and other aromatic hydrocarbons), water vapor, hydrogen sulfide (H<sub>2</sub>S), residual solids, and other trace species (HCN, NH<sub>3</sub>, and HCl). The specific fractions of the various species obtained may depend on process conditions and on the environment (inert, steam) prevailing during gasification. Other inorganic materials present in biomass such as Si, Al, Ti, Fe, Ca, Mg, Na, K, P, S, and Cl may also be converted to gaseous species.

Upon heating, the biomass dries up, until it reaches 120 °C. Volatiles are produced until it reaches 350 °C, and the resulting char is gasified above 350 °C. Therefore, it is customary to classify the entire gasifier process into three steps: drying, devolatilization, and gasification.<sup>55,80</sup> Gasification itself is a combination of pyrolysis and oxidation reactions. Chemical species are heated up to 500–900 °C in the presence of air, steam, CO<sub>2</sub>, or other components. Heat to drive the process is generated either outside the unit or in the same unit via exothermic biomass combustion.

Evans and Milne<sup>81</sup> observed three major reaction regimes during the gasification process identified as primary, secondary, and tertiary regimes. During the primary stage below 500 °C of gasification, solid biomass forms gaseous H<sub>2</sub>O, CO<sub>2</sub>, oxygenated vapor species, and primary oxygenated liquids. The primary oxygenated vapors and liquids include cellulose-derived molecules (such as levoglucosan, hydroxyacetalddehyde), their analogous hemicellulose-derived products, and lignin-derived methoxyphenols. No chemical interactions were observed among

the organic compounds during primary pyrolysis reactions, which are substantially free of secondary gas-phase cracking products. Primary pyrolysis vapors are of rather low molecular weight, representing monomers and fragments of monomers. However, the aromatization process starts at 350 °C and continues at higher temperatures.<sup>82</sup>

During the secondary stage, which takes place from 700 to 850 °C, the primary vapors and liquids form gaseous olefins, CO, CO<sub>2</sub>, H<sub>2</sub>, H<sub>2</sub>O, and condensable oils such as phenols and aromatics. The composition of tars formed during this phase is reported in Table 3. Gases and remaining tars undergo other secondary reactions such as water gas shift, methanation, steam reforming, and cracking. However, these reactions in which catalysts are not present are generally too slow. The only exception is the water gas shift reaction.<sup>83</sup> Further heating of evolved chemical species occurs from 850 to 1000 °C, resulting in a reaction phase where secondary products form, consisting of CO, CO<sub>2</sub>, H<sub>2</sub>, H<sub>2</sub>O, and polynuclear aromatics (PNA). These compounds include methyl derivatives of aromatics such as methyl acenaphthylene, methyl naphthalene, toluene, and indene. Some other products such as benzene, naphthalene, acenaphthylene, anthracene, phenanthrene, and pyrene condense to form a liquid tar phase.<sup>83</sup>

According to Evans et al.,<sup>84</sup> the composition of the tars changes as the temperatures increases in the following order: mixed oxygenates → phenolic ethers → alkyl phenolics → heterocyclic ethers → polycyclic aromatic hydrocarbons → larger polycyclic aromatic hydrocarbons.

However, an analysis of the high-temperature tar derived from cellulose showed levoglucosan to be a primary component.<sup>11</sup> The time of the gasification has significant effects on tar conversion. Longer vapor residence times at pyrolysis temperatures yields more secondary vapor-phase cracking leading to additional gases, water, formic acid, acetic acid, and other low-molecular-weight products.<sup>9,85</sup> Soot and coke are formed during these secondary and tertiary processes. Coke forms from thermolysis of liquids and organic vapors. The homogeneous nucleation of the intermediate chemical species, produced at high temperature, yields soot in the gas phase.

During gasification, the inorganic components of the biomass are usually converted into ash, which is removed from the bottom of the gasifier (bottom ash), or into fly ash, which leaves with the product gas. The composition of the ash includes CaO, K<sub>2</sub>O, P<sub>2</sub>O<sub>5</sub>, MgO, SiO<sub>2</sub>, SO<sub>3</sub>, Na<sub>2</sub>O, and residual carbon. Volatile halogen elements and alkali elements are mainly found in wet scrubber ash and in fly ash, whereas Si, Ni, Pb, Zn, Cr, Cd, K, S, Mn, and Cu elements are typically contained in the ash separator exit, enriched with heavy metals.<sup>13</sup>

Among biomass formed products, char retains the morphology of the original lignocelluloses. Char is formed through cross-linking reactions via condensation and water loss<sup>86</sup> with slow pyrolysis yielding more char.<sup>87</sup> The char yield decreases rapidly with increasing temperature until 400 °C is reached. As the temperature increases, the char becomes progressively more aromatic and high in carbon. This is due to the removal of hydroxyl, aliphatic C–H bonds and carbonyl and olefinic C=C groups. The release of volatile matter opens spaces in the char pore structure at the higher gasification temperatures. Higher temperatures may also lead to char softening, melting, and fusion. The shrinkage of the carbon structure may take place above 500 °C, which is concurrent with the aromatization process.<sup>82</sup> Char that is formed from the initial pyrolysis and from secondary

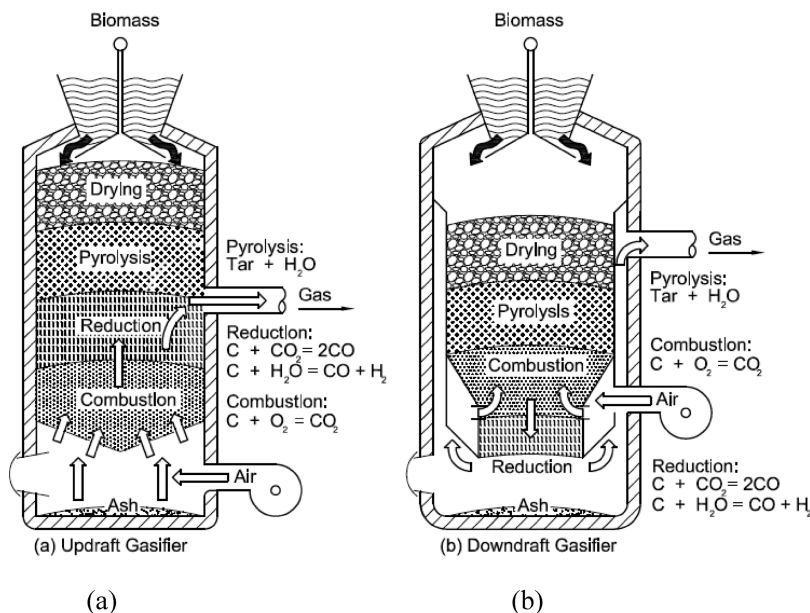


Figure 5. Schematic of (a) updraft and (b) down draft gasifier. Adapted from<sup>75</sup>.

tar reactions continues to pyrolyze and react with steam (i.e., the carbon/steam reaction), producing additional permanent gases.

## 2.5. Design of Gasifiers

Gasifiers can be divided into two principal types: fixed beds and fluidized beds, with variations within each type. A third type, the entrained suspension gasifier, has been developed for the gasification of finely divided coal particles (<0.1–0.4 mm) only. This type of gasifier is not recommended for fibrous materials such as wood, which makes the process largely unsuitable for most biomass materials.<sup>5</sup>

**2.5.1. Fixed-Bed Gasifiers.** Fixed-bed gasifiers are the oldest and historically most common reactors used to produce syngas. Fixed-bed gasifiers are widely used and studied because of their simplicity in construction and operation. The term “fixed bed” is in fact a misnomer given to these units as the unreacted biomass moves very slowly with respect to the fast evolving gases.

In the last two decades, however, large-scale (>10 MW) fixed-bed gasifiers have lost a part of their industrial market appeal. Yet, small-scale (<10 MW) fixed-bed gasifiers with a relatively high thermal efficiency and minimal pretreatment of the supplied biomass have maintained a commercial interest, especially in the area of locally based power generation.

Depending on the direction of airflow, fixed gasifiers are classified as updraft, downdraft, or cross-flow.<sup>56</sup> Each of these gasifiers, as illustrated in Figures 5a and 5b, display a different distribution of gasification zones. In updraft gasifiers and downdraft gasifiers, the gas composition by volume is typically in the following ranges: CO (20–30%), H<sub>2</sub> (5–15%), CH<sub>4</sub> (1–3%), and CO<sub>2</sub> (5–15%).<sup>88</sup>

**2.5.1.1. Updraft Gasifier.** An updraft gasifier is a gasifier with four identifiable zones: (a) an upper drying zone, (b) an upper-middle pyrolysis section, (c) a lower-middle reduction zone, and (d) a lower combustion zone. In an updraft gasifier, the biomass is introduced at the top of the gasifier while air is fed at the bottom of the unit via a grate (Figure 5a).

In the top gasifier section, the fed biomass is dried. Following drying, the biomass moves slowly downward reaching the pyrolysis

zone, where the volatile species are released and considerable quantities of tars are formed. After pyrolysis, volatiles are converted into permanent gases in the reduction zone. The residual biomass finally reaches the near grate zone where the solid char, and the remaining biomass, are combusted at 1000 °C. Once char combustion with air is complete, the formed ash falls through the grate.

In updraft gasifiers, the hot gases emerging from the combustion zone move upward in the unit, interacting with the falling unconverted biomass in the reduction zone. Tar also condenses partially in the pyrolysis zone, on the descending biomass, and/or leaves the gasifier together with the permanent gases.

Thus, in the updraft gasifier, biomass may have a favorable filtering effect producing permanent gases with low tar content. The temperature in the gasification zone can also be controlled by cofeeding steam and air or by humidifying the air. Formed gases are cooled down to 200–300 °C. Because of the relatively low temperature of the gas leaving the unit, the overall updraft gasifier energy efficiency is quite high.<sup>89</sup>

**2.5.1.2. Downdraft Gasifier.** A downdraft gasifier as shown in Figure 5b is a gasifier unit with four distinct zones: (a) upper drying zone, (b) upper-middle pyrolysis section, (c) lower-middle oxidation zone, and (d) lower reduction zone. Fed biomass is dried in the upper section. Following this, the biomass moves downward to the upper-middle zone, enabling the devolatilization and the tar reforming reactions to take place. Next, unconverted tars and gases evolve toward the oxidation zone, where combustion takes place at 1000–1400 °C. Formed chemical species finally move through a reduction zone where the H<sub>2</sub> and CO contents are enriched.

The product gas in a downdraft gasifier contains a low concentration of particulates and tars (~1 g/Nm<sup>3</sup>) as most of the tars are combusted in the gasifier section. Remaining tars in a downdraft gasifier are almost exclusively the less-reactive tertiary tars. The downdraft gasifier is ideal when a clean syngas gas with a low content of tar and particulates is desired.<sup>90</sup>

The disadvantages of this type of gasifier include difficulties in handling biomass with high moisture and high ash contents. Downdraft gasifiers display as well a relatively low overall thermal

efficiency. Downdraft gasifiers' low thermal efficiency is the result of produced gases leaving the unit at high temperature. To compensate for this, heat from the hot gases is often transferred to the gasifying agent, yielding a thermal unit efficiency at par with updraft gasifiers.

**2.5.1.3. Cross-flow Gasifier.** In a cross-flow gasifier, the biomass fed at the top of the unit moves downward while air is introduced from the opposite side of the unit. Gases are withdrawn from the upper side of the unit at about the same level where the biomass is fed. A hot combustion/gasification zone forms around the air entrance, with pyrolysis and drying zones being formed higher up in the vessel. Ash is removed at the unit bottom, and the temperature of the gas leaving the unit is about 800–900 °C. As a result, low overall energy efficiency with a gas having high tar content is expected in cross-flow gasifier units.

**2.5.2. Fluidized-Bed Gasifiers.** Among the technologies that can be used for biomass combustion, fluidized beds are promising given their flexibility and high efficiency. Fluidized-bed (FB) gasification has been used extensively for coal gasification for many years. Its advantage over fixed-bed gasifiers is the uniform temperature distribution achieved in the gasification zone. This temperature uniformity is accomplished using a bed of fine granular material (e.g., sand) into which air is circulated, fluidizing the bed. Intense bed fluidization promoting solid circulation also favors the mixing of the hot bed material, the hot combustion gases, and the biomass feed. Fluidized beds are used for a broad variety of fuels. This flexibility with respect to different fuels is actually another critical advantage of fluidized beds.<sup>91</sup> Furthermore, a typical intermediate tar level of 10 g/Nm<sup>3</sup> is achieved in fluidized beds. Tar created is formed by a blend of secondary and tertiary tars.<sup>5</sup>

Loss of adequate fluidization known as defluidization due to particle agglomeration is a major problem in fluidized-bed gasifiers operated above 800 °C. The most common problem found in fluidized beds as a preamble to defluidization in commercial-scale installations is the “coating-induced” agglomeration of the fine granular material forming the bed. During reactor operation, a coating is formed on the bed sand particle surfaces. At certain critical coating thicknesses and/or temperature levels, the undesirable sintering of the bed particles is caused by biomass sodium content. Sodium lowers the melting point of the silicates and aluminosilicates of the particles.<sup>92</sup> Agglomeration associated with fluidized bed gasifiers is still a major issue when used to gasify certain herbaceous biofuels. However, there are successful solutions that have been reported for other biomass feedstocks.<sup>7</sup> These solutions are mainly based on lowering and controlling the bed temperature.

Two main types of fluidized-bed gasifiers are in current use. These are the following: (a) a circulating fluidized bed and (b) a bubbling bed. A third type of FB gasifier, which is an internally circulating bed that combines the design features of the other two types, is currently being investigated at the pilot-plant scale.

**2.5.2.1. Circulating Fluidized-Bed Gasifier.** Circulating fluidized-bed gasifiers are able to cope with high-capacity biomass throughputs and are used in the paper industry for the gasification of bark and other forestry residues. The bed material is circulated between the reaction vessel and a cyclone separator, where the ash is removed and the bed material and char are returned to the reaction vessel. Circulating fluidized-bed gasifiers can be operated at elevated pressures. The gases produced are delivered at gas turbine operating pressures without requiring further compression.

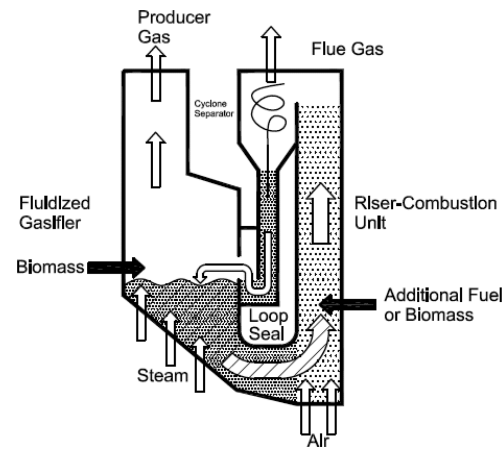


Figure 6. Schematic of the dual fluidized-bed steam gasification system. Adapted with permission from ref 96. Copyright 2009.

Viking Company has proposed a 500 kW LTCFB gasifier (low-temperature circulating fluidized bed) specially developed for fuels with high alkali contents. Until now, it has been successfully operated on straw containing >12 wt % ash, pig manure, and chicken litter.

There are still issues concerning circulating fluidized-bed gasifiers as follows: (i) particle content in the raw gas is close to the one in fixed beds while tar formed is higher and (ii) investments and operating costs are higher than in fixed-bed gasifiers.<sup>93,94</sup>

**2.5.2.2. Bubbling Fluidized-Bed Gasifier.** The bubbling FB gasifier consists of a vessel with a grid at the bottom through which air is introduced. Above the grid there is a moving bed of fine-grained material into which the prepared biomass feed is introduced. Regulation of the bed temperature to 700–900 °C is maintained by controlling the air/biomass ratio. The biomass is pyrolyzed in the hot bed, forming char, gaseous compounds, and tar. The high molecular weight tar is cracked by contact with the hot bed material, giving a product gas with a lower tar content (<1–3 g/Nm<sup>3</sup>). For steam gasification without a catalyst, the tar produced in the gasifier is ~12 wt % of the fed cellulose. The main components of tar are celotriosan, cellobiosan, and levoglucosan.<sup>95</sup>

**2.5.2.3. Dual Fluidized-Bed Gasifier.** There is another type of technology called the dual fluidized bed (DFB), which has been developed in Austria using steam as the gasification agent and providing the heat for the gasification reactor by circulating the bed material.<sup>96</sup> As shown in Figure 4, the biomass enters a bubbling fluidized-bed gasifier where the steps of drying, devolatilization, and partially heterogeneous char gasification take place at temperatures of 850–900 °C. Residual biomass char leaves the gasifier together with the bed material through an inclined, steam-fluidized chute toward the combustion reactor. The combustion zone (riser), designed for high solid transport rates, serves to heat up the bed material. After particle separation from the flue gas in a cyclone, the hot bed material flows back to the gasifier via a loop seal.<sup>97</sup> Dual circulating fluidized beds have been commercially demonstrated in coal-fired power stations.<sup>98,99</sup> Gasification in an integrated plant for the production of synthetic natural gas using the dual circulating-bed gasifier of Figure 6 is considered to be advantageous given the higher energy conversion from the produced syngas.<sup>100</sup>

**2.5.2.4. External Circulating Concurrent Moving-Bed Gasifier.** More recently, a new process of biomass gasification designated as

the external circulating concurrent moving-bed gasifier or ECCMB system has been proposed. This system is composed of a moving bed with gasification and combustion zones. A circulation loop allows the transport of bed material and, as a result, heat transfer between the two zones. The char deposited on the catalyst burns off in the combustion zone, and as a result, the catalyst is continuously regenerated. The char combustion also provides the energy for the endothermic steam gasification in the gasification zone. A lab-scale facility was established to demonstrate this process concept, where steam gasification of biomass and combustion of the produced char can occur simultaneously. A H<sub>2</sub> content of 53.3 mol % and a tar yield of 0.7 g/Nm<sup>3</sup> were obtained in a unit operated at a S/B ratio (steam/biomass mass ratio) of 0.4 g/g and at a temperature of 800 °C using a calcined olivine catalyst. The obtained results show that this new concept of biomass gasification for the production of hydrogen-rich gas is feasible. It also appears that concurrent biomass and catalyst transport in the gasification zone enhances the process and reduces tar formation.<sup>101</sup>

### 2.5.3. Advantages/Disadvantages of the Different Gasifying Reactors.

Listed below are key criteria that need to be addressed when selecting a gasifier reactor:

- Capital costs,
- Operating and maintenance,
- Robust gasifier configuration without moving parts, and
- As much as possible, avoidance of feedstock preparation such as drying, separation, size reduction, or pelletization.

A reported comparison between fixed-bed and fluidized-bed reactors based on technology, use of material, use of energy, environment, and economy shows that there are niche applications for these two systems.<sup>102</sup> Selection of a particular gasifier type and its design will require, however, a close scrutiny of a number of other factors such as the properties of the feedstock (both chemical and physical), the quality of product gas required, the heating method, and the various operational variables involved.<sup>103</sup>

The features of a fluidized-bed gasifier that make it appear less attractive are a more complex design and operation, as well as the additional energy expenses required for biomass particle size reduction. Particle size reduction also entails the formation of dust. Catalyst attrition may be a major issue limiting catalyst utilization in fluidized-bed reactors. Materials such as dolomite and many conventional, high surface area metal oxide supports may experience high attrition. High-strength materials, such as olivine and specially designed catalysts, are recommended. The product gas may also contain tars requiring a gas cleaning external to the gasifier. It is expected that high plant costs make fluidized-bed gasification economical at the 5–10 MW scale. In comparison to fluidized-bed gasifiers, fixed-bed gasifiers have no or very few moving parts and, as a result, are very adaptable for the production of low calorific value gas in small-scale power generation stations with gas turbines.<sup>75</sup>

Carbon conversion, product gas composition, tar formation, and tar reduction are all important biomass gasification performance indicators. The most important parameters affecting these performance indicators are temperature, pressure, gasifying agent, catalyst and additives, equivalence ratio (ER), and residence time. For instance, homogeneous bed temperature profile and intense mixing, as achieved in fluidized beds, are of utmost importance to avoid disturbances in the operation of the gasifier.<sup>104</sup>

Another interesting proposal to extend Ni catalyst time-on-stream is to employ a combination of gasifiers: a fixed guard bed followed by a fluidized bed.<sup>86</sup> The fixed guard bed is packed with

an inexpensive material, such as dolomite, to precondition the biomass-derived primary synthesis gas. The use of a fixed guard bed helps to reduce the content of tars and impurities in the primary synthesis gas, such as sulfur, chlorine, and hydrogen sulfide. The primary synthesis gas, clean of contaminants and impurities, is sent to a fluidized-bed reactor containing a Ni catalyst for further purification of the syngas composition.

## 2.6. Gasifier Operating Conditions

**2.6.1. Equivalence Ratio.** Previous experimental investigations<sup>48,50,51,105–108</sup> have demonstrated the important effect of the steam/biomass ratio on the product gas composition.

The equivalence ratio (ER) is a key parameter that considers the actual air/biomass ratio divided by the stoichiometric air/biomass ratio as

$$\text{ER} = (F_{\text{oxidant}}/F_{\text{biomass}})/(F_{\text{oxidant, stoichiometry}}/F_{\text{biomass}}) \quad (1)$$

with stoichiometric oxidation or complete combustion taking place at ER = 1.<sup>109</sup>

The ER strongly influences the type of gasification products. This is very crucial because a high ER value results in a lower concentration of H<sub>2</sub> and CO as well as in a higher CO<sub>2</sub> content in the product gas. Thus, a higher ER decreases the heating value of the syngas. Increasing the ER also has a beneficial effect on reducing tar formation given the greater availability of oxygen to react with volatiles. This phenomenon is more significant at higher temperatures. On the other hand, an increase in the steam/biomass ratio is expected to produce a higher hydrogen fraction as a result of the water gas shift reaction. In addition, excess steam often drives the cracking of higher hydrocarbons and reforming reactions.<sup>110</sup>

Lv et al.<sup>111</sup> divided biomass gasification into two stages based on the ER. In the first stage, the ER varied from 0.19 to 0.23. At this ER value, the gas yield increased from 2.13 to 2.37 Nm<sup>3</sup>/(kg biomass) and the lower heating value (LHV) of the gas was augmented from 8817 to 8839 kJ/Nm<sup>3</sup>. In the second stage, the ER ranged from 0.23 to 0.27 and the heating value decreased as the ER increased, with this being the result of the influence of combustion in the gasification products. Garcia-Ibanez<sup>112</sup> reported that the maximum amount of H<sub>2</sub> (9.3 vol %) occurred at an ER of 0.59. When the ER range was between 0.59 and 0.73, this had a slight effect on the hydrocarbon content. The increase of the steam/biomass ratio also had a positive effect on the life of the catalyst.<sup>113</sup>

However, according to Zhou et al.,<sup>114</sup> ER does not significantly influence the concentration of nitrogen-containing products in biomass gasification. A slight increase in NH<sub>3</sub> was observed when the ER was increased from 0.25 to 0.37 at 800 °C in sawdust gasification.

Nevertheless, the steam/biomass ratio provides an upper limit set by gasification stoichiometry. Exceeding this limit yields excess steam and H<sub>2</sub>O in the product gas. The energy associated with excess steam and the enthalpy losses resulting from the unnecessary production of this steam need to be considered in the system energy balances. Such issues demonstrate the importance of selecting an optimal steam/biomass ratio in biomass steam gasification for achieving high process efficiency.

Temperature, as described in Figure 7, is closely related to changes in ER and feeding rate. The bed temperature increased linearly with ER when the feeding rate was kept constant. On the other hand, higher feeding rates yielded a lower bed temperature at constant ERs.

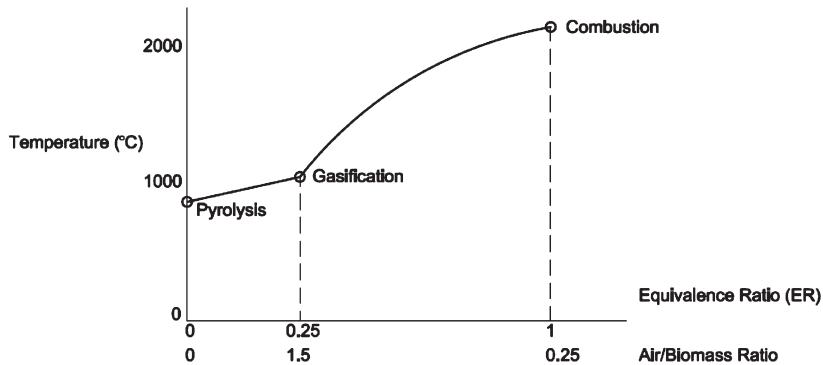


Figure 7. Equivalence ratio. Adapted with permission from <http://www.woodgas.com/EquivalenceRatioDiagram.pdf>.

The water and volatile content of the biomass had an influence on the operation of the gasifier. For instance, increases in water content up to 15% resulted in larger ERs and gas yields, whereas water content above 15% caused anomalous temperature fluctuations.<sup>115</sup> Happing et al.<sup>116</sup> observed that a lower heating value (LHV) of gas and higher amount of tars were obtained from biomass with a high volatile matter. In the following section, effects of the main operating variables are reviewed.

**2.6.2. Operating Temperature.** Researchers have conducted extensive studies reviewing the influence of temperature on tar production during biomass gasification.<sup>117</sup> To achieve a high carbon conversion of the biomass and a low tar content, a high operating temperature (>800 °C) in the gasifier is recommended. With the increase in temperature, combustible gas content, gas yield, hydrogen, and heating value all increased significantly, while the tar content decreased sharply. Although this showed that higher temperatures are favorable for biomass gasification,<sup>116,118,119</sup> from an overall process perspective, reduction of ash agglomeration requires lower temperatures. In practice, this may limit gasification temperatures up to 750 °C.<sup>19,27</sup>

Moreover, Mahishi and Goswami<sup>120</sup> reported that the hydrogen at chemical equilibrium initially increased with temperature, reached a maximum, and then gradually decreased at the highest temperatures. Temperature affects not only the amount of tar formed but also the composition of tar by influencing the chemical reactions involved in the gasification network.<sup>121</sup> To produce a relatively clean gas by increasing temperature, several operational strategies are reported in the literature. Fagbemi et al.<sup>122</sup> showed that tar yields were augmented first while temperature rose up to 600 °C and then dropped after this temperature was surpassed. At higher temperatures, primary  $C_nH_m$  were less significant and secondary reactions (i.e., tar cracking) prevailed. This led to considerable tar decomposition.<sup>43</sup> In the combustion zone of the gasifier, reactions between char and oxygen played a more dominant role, however.<sup>123</sup> Therefore, several factors including tar content, gas composition determining gas heating value, and char conversion should all be taken into consideration and weighted carefully in the selection of the gasifier operating temperature.

**2.6.3. Operating Pressure.** Several researchers have investigated pressurized biomass gasification.<sup>124,125</sup> When the pressure was increased, a reduction in the amount of light hydrocarbons (LHC, lower than naphthalene) and tars with larger ERs were observed. This occurred with 100% carbon conversion. Although the total amount of tar decreased with greater pressures, the fraction of polycyclic aromatic hydrocarbons increased.

**2.6.4. Gasifying Agents.** Gasification under different atmospheres such as air, steam, steam–oxygen, and carbon dioxide has been reported in the literature. In general, the gasifier atmosphere determines the calorific value of the syngas produced. When one uses air as the gasifying agent, a syngas with low heating value is obtained. This is mainly due to the syngas dilution by the nitrogen contained in air.<sup>126–130</sup> However, if one uses steam or a combination of steam and oxygen, a syngas with a medium calorific value is produced.<sup>49,51,128,131–137</sup> In addition, the combined use of steam and air gives much higher H<sub>2</sub> yields than with air alone. This also helps to reduce the energy required for the process, which is normally provided by combusting a fraction of the biomass.

**2.6.5. Residence Time.** Residence time has a significant influence on the amount and composition of the produced tars. According to Kinoshita et al.,<sup>138</sup> the fraction of oxygen-containing compounds tends to decrease by increasing residence time. Furthermore, yields of one and two aromatic ring compounds (except benzene and naphthalene) decrease with residence time, whereas those of three- and four-ring species increase. Corella et al.<sup>139</sup> observed a decrease in the total tar content when the space time was augmented in biomass gasification with a bed of dolomite.

## 2.7. Advantages and Technical Challenges for Biomass Gasifiers

The advantages and technical challenges of different gasifying agents, gasifier designs, and operations for syngas production are summarized in Table 5. Overall, it can be observed that fluidized gasifiers with their exceptional temperature control offer unique opportunities in the area of catalytic gasification of biomass for the development of highly efficient biomass gasifier units.

## 3. CATALYSTS FOR STEAM GASIFICATION OF BIOMASS

A considerable volume of research has been conducted with the goal of developing biomass gasification processes in the recent years. However, a serious issue for the broad implementation of this technology is how to deal with the generation of unwanted contaminants (e.g., tar, coke-on-catalyst, particles, nitrogen compounds, and alkali metals).<sup>140</sup> Tar is a complex mixture of condensable hydrocarbons including single-ring to 5-ring aromatic compounds. It also includes oxygen-containing hydrocarbon species, which cause blockage and corrosion and reduce overall efficiency of the gasifier.<sup>9</sup> For commercial applications, tar components must be typically limited to <1 g/m<sup>3</sup> of gas at STP conditions.

Tar can be converted thermally. High gasification temperature reduces the formation of tar; but high energy consumption (i.e.,

**Table 5.** Advantages and Technical Challenges of Different Gasifier Designs, Gasifying Agents, and Operations for Synthesis Gas Production<sup>66</sup>

	main advantages	main technical challenges to overcome
Gasifier design		
fixed/moving beds	<ul style="list-style-type: none"> <li>1 involves a simple and reliable design</li> <li>2 suitable for wet biomass gasification</li> <li>3 entails favorable economics at small scale</li> </ul>	<ul style="list-style-type: none"> <li>1 operates at longer residence time</li> <li>2 operates with nonuniform temperature distribution</li> <li>3 yields high char and/or tar contents</li> <li>4 yields a low cold gas energy efficiency</li> <li>5 adequate for low biomass processing capacity</li> </ul>
fluidized bed	<ul style="list-style-type: none"> <li>1 operates with short residence time</li> <li>2 involves a high biomass processing capacity</li> <li>3 provides a uniform temperature distribution</li> <li>4 yields low char and/or tar contents</li> <li>5 has a high low cold gas energy efficiency</li> <li>6 involves reduced ash-related problems at low—medium temperatures</li> </ul>	<ul style="list-style-type: none"> <li>1 yields high particulate dust concentrations in syngas</li> <li>2 displays favorable economics on a medium to large scale only</li> </ul>
Gasifying agents		
air	<ul style="list-style-type: none"> <li>1 provides partial combustion for gasification heat supply</li> <li>2 yields moderate char and tar contents</li> </ul>	<ul style="list-style-type: none"> <li>1 provides a low heating value (4–6 MJ/Nm<sup>3</sup>) with large amount of N<sub>2</sub> in the produced syngas (e.g., &gt;50% by volume)</li> <li>2 yields a ER usually between 0.2 and 0.4</li> </ul>
steam	<ul style="list-style-type: none"> <li>1 yields a high heating value syngas (13–20 MJ/Nm<sup>3</sup>)</li> <li>2 yields a H<sub>2</sub>-rich syngas (e.g., &gt;50% by volume)</li> </ul>	<ul style="list-style-type: none"> <li>1 requires indirect or external heat supply for gasification</li> <li>2 yields a high tar content in syngas</li> <li>3 requires catalytic tar reforming</li> </ul>
carbon dioxide	<ul style="list-style-type: none"> <li>1 yields a high heating value syngas</li> <li>2 yields high H<sub>2</sub> and CO in syngas and low CO<sub>2</sub> in syngas</li> </ul>	<ul style="list-style-type: none"> <li>1 requires indirect or external heat supply</li> <li>2 requires catalytic tar reforming</li> </ul>
Gasifier operation		
temperature increase	<ul style="list-style-type: none"> <li>1 yields reduced char and tar content</li> <li>2 yields reduced methane in syngas</li> <li>3 yields increased carbon conversion</li> <li>4 yields increased syngas heating value</li> </ul>	<ul style="list-style-type: none"> <li>1 yields a decreased energy efficiency</li> <li>2 increases ash-related problems</li> </ul>
increase of pressure	<ul style="list-style-type: none"> <li>1 yields low char and tar content</li> <li>2 yields a compressed syngas required for downstream utilization</li> </ul>	<ul style="list-style-type: none"> <li>1 increases uncertainty given the limited design and operational experience</li> <li>2 yields more expensive small scale gasifier</li> </ul>
increase of ER	<ul style="list-style-type: none"> <li>1 yields low char and tar contents</li> </ul>	<ul style="list-style-type: none"> <li>1 decreases heating value of syngas</li> </ul>

high production cost for syngas) makes the process economically unviable.<sup>141</sup> Even at temperatures in excess to 1000 °C, tar cannot be removed completely. Moreover, it is highly desirable to keep the operating temperature of the gasifier below 750 °C, to prevent ash agglomeration. Ash frequently contains CaO, K<sub>2</sub>O, P<sub>2</sub>O<sub>5</sub>, MgO, SiO<sub>2</sub>, SO<sub>3</sub>, and Na<sub>2</sub>O that can sinter, agglomerate, deposit on surfaces, and contribute to erosion and corrosion of the gasifier. Furthermore, alkaline metals react readily in the gasifier with silica forming silicates or with sulfur-producing alkali sulfates, leaving a sticky deposit and in many instances causing bed sintering and defluidization.<sup>14–16</sup>

Catalytic reforming can be used to convert tar into gaseous products. For more than three decades,<sup>9,10,20,140,142,143</sup> it has been the most promising method for tar removal, avoiding costly tar disposal. The use of catalysts during biomass gasification promotes char gasification, changes the product gas composition, and reduces the tar yield obtained when the gasifier is operated at lower temperatures. Moreover, the addition of dopants to the Ni-based catalyst such as Fe, Mg, Mn, Ce, Pt, Pd, Rh, and Ru influences not only the gas composition but also the heating value of the product gas.<sup>144,145</sup>

Thus, given the value of catalysts for gasification, relevant research has been done with the goal of developing stable and

highly active catalysts for biomass gasification producing high-quality synthesis gas and/or hydrogen free of tars. Significant amounts of study have been carried out using dolomite, olivine, alkali, and noble metal catalysts for this purpose.

Catalysts have been employed directly in the gasifier, and in these cases they are referred to as *primary catalysts*.<sup>10,20–26</sup> These primary catalysts such as dolomite, calcined dolomite, olivine, and Ni/Al<sub>2</sub>O<sub>3</sub> promote several important chemical reactions such as water gas shift and steam reforming. Thus, there is the opportunity with primary catalysts to minimize tars and increase both hydrogen and CO<sub>2</sub>, avoiding altogether complex downstream tar removal operations.<sup>24</sup> However, catalysts in the gasifier, particularly the Ni-based catalysts, may be affected by deactivation due to carbon deposition on the catalyst surface.<sup>143,146</sup> Furthermore, the addition of active materials to the bed also helps prevent the solid agglomeration tendencies and subsequent choking of the bed.

In spite of the challenges, the use of primary catalysts, in the context of biomass gasification, is gaining much attention nowadays as they reduce the need for expensive downstream operations.<sup>10</sup> Another possible alternative is to have a catalytic process in a reactor placed downstream from the gasifier. In this reactor, product gases are further processed using secondary catalysts.<sup>20</sup> Typical materials that are used as *secondary catalysts* are dolomite and nickel-based formulations. These catalysts decrease the tar content of the product gas in the 750–900 °C range.<sup>20,143,146–150</sup> Secondary catalysts are effective for hot gas cleaning with the overall cost of the gasification process increasing significantly.<sup>141</sup> According to Asadullah et al.,<sup>151</sup> when some Rh/CeO<sub>2</sub> secondary catalysts are used, the formation of CH<sub>4</sub> and CO<sub>2</sub> may in cases increase significantly and the formation of CO and H<sub>2</sub> may be reduced.

Catalytic biomass gasification is a complex process that includes numerous chemical reactions steps such as pyrolysis, steam gasification, and water gas shift reaction.<sup>152</sup> Contributions in the development of stable and efficient biomass gasification catalysts are reviewed in the next section of this article.

### 3.1. Dolomite, Olivine, and Alkali Metal-Based Catalysts

The use of dolomite, a magnesium ore with the general formula MgCO<sub>3</sub> CaCO<sub>3</sub>, as a primary and/or secondary catalyst in biomass gasification has attracted much attention because it is a cheap disposable catalyst that can significantly reduce the tar content of the product gas from a gasifier. The main issue with dolomite is its fragility, as it is soft and quickly attrites in fluidized beds under prevalent high-turbulence conditions.<sup>10</sup>

Dalai et al.<sup>153</sup> studied the performance of a CaO catalyst by varying the catalyst loading from 0 to 8.9 wt % during temperature-programmed gasification (TPG) and constant-temperature gasification (CTG). Experiments showed that the use of CaO as a primary catalyst reduced the maximum gasification temperature by 150 °C. In addition, the total fuel produced and the hydrogen and carbon yielded were significantly increased with CaO impregnated in cellulose, cedar, and aspen. Furthermore, the rate and the cumulative production of H<sub>2</sub> from CaO impregnated in cedar and aspen were higher than those from CaO impregnated in cellulose both for catalytic as well as for noncatalytic TPG and CTG.

Aznar et al.<sup>52</sup> conducted parametric studies using dolomite as a tar cracking catalyst. The feedstock was composed of blends of plastic waste mixed with pine wood sawdust and coal at flow rates of 1–4 kg/h. Operating variables studied were gasifier bed

temperature (750–880 °C), equivalence ratio (0.30–0.46), feedstock composition, and the influence of secondary air fed into the freeboard. As a result, a gas with medium hydrogen content (up to 15% dry basis) and low tar content (<0.5 g/m<sup>3</sup>) was obtained. Additionally, these authors found that the injection of secondary air into the freeboard reduced tar content by 50%, down to 5 g/m<sup>3</sup>. Under these conditions, a clean gas was obtained.

A few studies have been done recently into the catalytic activity of olivine and dolomite for tar elimination. Hu et al.<sup>154</sup> tested calcined olivine and calcined dolomite as catalysts in a fixed-bed reactor. Results showed that the catalytic activities of calcined catalysts were higher than the untreated ones. A similar system was used by Devi et al.,<sup>155</sup> who observed that, in the case of untreated olivine and calcined dolomite, tar conversion increased when temperature reached 800 to 900 °C. These authors found that water-soluble heterocyclic compounds could be 100% converted at 900 °C. Additionally, the conversion of heavy polyaromatics increased from 48% to 71% using 17 wt % untreated olivine mixed with sand at 900 °C, whereas the conversion of heavy polyaromatics reached up to 90% with 17 wt % of calcined dolomite. Furthermore, a total tar amount of 4.0 g/m<sup>3</sup> could be reduced to 1.5 and 2.2 g/m<sup>3</sup> using calcined dolomite and olivine, respectively.

Xu et al.<sup>156</sup> demonstrated that, for atmospheric gasification of biomass, CaO could also be used as an effective CO<sub>2</sub> capture material, provided that the reaction temperature was selected appropriately. It was shown that, at temperatures below 730 °C, the CaO captured CO<sub>2</sub>, yielded a CO<sub>2</sub> in the product gases that was below 10 vol %, and increased, as a result, the heating value of the product gases considerably. Furthermore, the addition of CaO increased the H<sub>2</sub> gas content and decreased the CO concentration, irrespective of the reaction temperature. This result corroborates the commonly known catalytic effect of CaO on CO<sub>2</sub> capture, water gas shift reaction, and tar reforming/cracking reactions.

Monovalent alkali metals of group 1A are all highly reactive and electropositive. Alkali metals, principally K and to a lesser extent Na, exist naturally in biomass and accumulate in the gasifier ashes. These alkali metals can have a significant impact during pyrolysis, forming a reactive char that enhances gasification.<sup>63,157–159</sup> Furthermore, the use of ash itself as a catalyst solves the problem of ash waste handling and gives an added value to the gasification by increasing the gasification rate and reducing the tar content in the produced gas. However, the major disadvantage of these ash-based catalysts is their potential activity losses due to particle agglomeration. Sutton et al.<sup>20</sup> reported several disadvantages in the direct addition of alkali metals, such as the difficult and the expensive recovery of the catalyst, which increased char content after gasification, and ash disposal problems. On the other hand, Lee et al.<sup>160</sup> found that the addition of Na<sub>2</sub>CO<sub>3</sub> while using nickel catalysts enhanced rice straw catalytic gasification and significantly increased the formation of permanent gases. The same authors found that the formation of permanent gases depended on the nature of the alkali metal carbonate used with the following reactivity order being assigned Na ≥ K > Cs > Li.

The highly beneficial use of activated alumina as a secondary catalyst for tar reduction comes from its high catalytic activity, comparable to dolomite,<sup>161</sup> although it deactivates by coke faster than dolomite. Juutilainen et al.<sup>162</sup> tested the activity of these catalysts also containing zirconia in the selective oxidation of tar and ammonia. This performance was compared with that of

nickel and dolomite catalysts. Synthesis gas with toluene as a tar model compound was used as feed in a fixed-bed tube reactor. The presence of oxygen, zirconia, and alumina-doped zirconia led to high toluene removal and ammonia conversions at temperatures below 600 °C. These catalysts were active for toluene oxidation below 700 °C and for ammonia oxidation below 650 °C. This showed that zirconia enhanced the oxidation activity, whereas alumina improved the oxidation selectivity. At higher temperatures, these  $\text{ZrO}_2/\text{Al}_2\text{O}_3$  catalysts performed even better. The authors concluded that both zirconia and alumina in catalyst formulations promoted toluene and ammonia conversions at lower temperatures.

### 3.2. Nickel-Based Catalysts

Among the transition metals (group VIII), nickel is the most widely used in the industry for steam and dry reforming reactions.<sup>163</sup> Commercially available nickel reforming catalysts have been used extensively for biomass gasification.<sup>142,143,147,148,164,165</sup> According to Aznar et al.,<sup>148</sup> under the conditions of catalytic gasification, nickel catalysts are more active for heavy hydrocarbon steam reforming (i.e.,  $\text{C}_n\text{H}_m + n\text{H}_2\text{O} \rightarrow n\text{CO} + ((n+m)/2)\text{H}_2$ ) than for light hydrocarbon steam reforming (i.e.,  $\text{CH}_4 + \text{H}_2\text{O} \rightarrow \text{CO} + 2\text{H}_2$ ). These nickel catalysts also promote water gas shift reaction ( $\text{CO} + \text{H}_2\text{O} \rightarrow \text{CO}_2 + \text{H}_2$ ) and are very effective in tar conversion. As a result, these nickel-based catalysts reduce tars while increasing  $\text{H}_2/\text{CO}$  ratio, improving synthesis gas quality. According to Olivares et al.,<sup>22</sup> nickel reforming catalysts display 8–10 times more reactivity than calcined dolomite.

**3.2.1. Catalyst Deactivation.** When using nickel-based catalysts, several deactivation mechanisms occur including poisoning by sulfur, chlorine, and alkali metals, sintering of Ni particles, and coke formation.<sup>11</sup> Ni-based catalysts deactivate rapidly due to coke formation and catalyst attrition. Coke formation is inherent to steam reforming processes. The high temperatures associated with reforming promote both higher hydrogen yields and undesirable coke formation. Coking in Ni-based steam reforming catalysts is reasonably well understood.<sup>166</sup> This process is the result of high-temperature reactions taking place both in the gas phase and on the catalyst surface. Tars and light and unsaturated hydrocarbons dissociate on catalyst metal surfaces to produce carbon deposits. They block the access to the catalyst pores, resulting in a loss of catalyst activity. The formed carbon may be gasified, may encapsulate on the catalyst surface, or may diffuse through the nickel to nucleate and precipitate, leading to the formation of carbon whiskers. Formation of carbon whiskers lifts the nickel crystallite from the catalyst surface, resulting in sintering. Therefore, nickel-based catalysts deactivate by carbon in two ways: (i) through the encapsulation of nickel crystallites by inactive carbonaceous layers of material and (ii) through the formation of inactive bulk nickel carbide phases.<sup>166–170</sup> Furthermore, there is a tendency for coke to be formed as a result of the increased unsaturation, molecular weight, and aromaticity of the feedstock.

Regarding coke formation, it can be minimized through the use of excess steam vis-a-vis the one required by gasification stoichiometry. In this respect, it is possible to estimate a minimum steam/carbon ratio required to avoid coke formation.<sup>171</sup> This provides a very useful guideline to establish the desired operating conditions. However, the practical negative effect of feeding extra steam is that it increases the overall energy costs for plant operation. Therefore and given the above-mentioned considerations, it is crucial to maintain as low a steam/C ratio as possible.<sup>166</sup>

If coke deposits on the catalyst surface at the same rate that it is removed by combustion, the catalyst surface remains clean. Thus, there is no catalyst deactivation and the catalyst is always effective in biomass gasification.<sup>143,172</sup> This is the ideal scenario that may happen in autothermal gasification where air fluidizes the catalyst and biomass bed, contributing to always keeping the catalyst free of coke. However, coke removal with combustion may also lead to metal oxide formation. The active metal component of the catalyst has to be reduced quickly to prevent poor catalyst activity and selectivity as well as limited catalyst life.

Ni-based catalysts are also prone to deactivation by sulfur. Struis et al.<sup>173</sup> investigated sulfur poisoning using several analytical techniques (temperature-programmed oxidation (TPO), X-ray photoelectron spectroscopy (XPS), and X-ray absorption spectroscopy (XAS)). To address these issues, Sato and Fujimoto<sup>174</sup> proposed a biomass gasification catalyst resistant to sulfur-containing species.

**3.2.2. Effect of Catalyst Support and Dopants.** The formulation of nickel catalysts may potentially involve the following components: (i) an active component (i.e., Ni), (ii) a second added component (i.e., a dopant or promoter), and (iii) a support phase. Generally, higher nickel content results in lower tar yield and higher  $\text{H}_2$  and CO yields. On the other hand, according to Bartholomew et al.,<sup>168</sup> the amount of nickel in the catalyst has a significant effect on the catalyst deactivation by coking. They suggested that a lower metal concentration results in stronger interaction with the support phase and higher metal dispersion. Thus, by controlling the metal addition, one can have a catalyst more resistant to deactivation by carbon fouling. Metal dispersion may be improved by addition of dopants or promoters. It has been proven that the activation and deactivation of nickel-based catalysts depend greatly on the type of support and the presence of additives/promoters. For instance, promoters may help to minimize the coke formation.

The support phase gives the catalyst mechanical strength and protection against severe conditions such as attrition and heat.<sup>11</sup> The pore structure of the support, the metal–support interactions, and the acidity–basicity of the support all significantly influence the metal dispersion, the metal crystallite size, and the carbon deposition on the catalyst surface, thus affecting the overall catalytic performance and catalyst coking resistance.<sup>175,176</sup> Baker et al.<sup>143</sup> also reported that the acidity of the support affects coke deposition and catalyst deactivation. For instance, higher acidity of the support materials favors tar cracking, leading to higher carbon buildup on the catalyst surface. On the other hand, Mark and Maier<sup>177</sup> reported that the pore structure or type of support did not affect the rate of dry reforming of methane. The role of the support is reported as stabilizing the metal surface, which, in turn, is responsible for catalyst activity.

Alumina-based materials are considered the primary support materials for most reforming catalysts. Gadalla and Bower<sup>178</sup> investigated the performance of  $\alpha\text{-Al}_2\text{O}_3$ - and  $\gamma\text{-Al}_2\text{O}_3$ -supported Ni catalysts for the reforming of methane with  $\text{CO}_2$ . They reported that the  $\text{Ni}/\alpha\text{-Al}_2\text{O}_3$  catalyst provided lower methane conversion than the  $\text{Ni}/\gamma\text{-Al}_2\text{O}_3$  catalyst, in spite of providing a more stable  $\alpha\text{-Al}_2\text{O}_3$  allotropic form given the smaller surface area of  $\alpha\text{-Al}_2\text{O}_3$ . They also showed that the  $\text{Al}_2\text{O}_3$  supports containing  $\text{MgO}/\text{CaO}$  were more stable. However, the addition of silica on  $\text{Ni}/\text{Al}_2\text{O}_3$  catalysts was not adequate given that it caused rapid deactivation. Wang and Lu<sup>175</sup> also reported higher conversion and lower deactivation

**Table 6.** Physical Properties, Catalytic Activities, and Deactivation Characteristics of Various Oxides-Supported Ni Catalysts<sup>175,176</sup>

catalyst			Ni crystallite size (nm)		CH <sub>4</sub> conversion @ 800 °C (%)	deactivation		sintering $d_2/d_1$
	support S <sub>BET</sub> (m <sup>2</sup> /g)	catalyst S <sub>BET</sub> (m <sup>2</sup> /g)	fresh ( $d_1$ )	used ( $d_2$ )		Conv <sub>3h</sub> /Conv <sub>10min</sub>	carbon deposition (g of C/g of Cat)	
Ni/La <sub>2</sub> O <sub>3</sub>	6.4	16.4	15.5	37.5	98	0.97	0.48	2.4
Ni/SiO <sub>2</sub>	290	239	12	21.8	96.2	0.87	0.068	1.8
Ni/TiO <sub>2</sub>	9.4	8.4	27.6		10			
Ni/ $\alpha$ -Al <sub>2</sub> O <sub>3</sub>	0.8	1.2	31.7	37.5	92.4	0.72	0.15	1.2
Ni/ $\gamma$ -Al <sub>2</sub> O <sub>3</sub>		157			95.8	0.95		
Ni/MgO	147.8	55.5			95.6	1.1	0.049	
Ni/CeO <sub>2</sub>	52	34			65	0.65	0.02	

rates for the Ni/ $\gamma$ -Al<sub>2</sub>O<sub>3</sub> catalyst when compared to the Ni/ $\alpha$ -Al<sub>2</sub>O<sub>3</sub> catalyst. They found that nickel aluminate (NiAl<sub>2</sub>O<sub>4</sub>) was formed due to the phase transformation of the  $\gamma$ -Al<sub>2</sub>O<sub>3</sub>-supported Ni catalyst during calcinations.

Nickel aluminate is difficult to reduce at lower temperatures. Temperatures higher than 800 °C are required for nickel aluminate reduction. As a result, the formation of nickel aluminate followed by its reduction has a negative impact on biomass gasification given the additional energy required. However, and once NiAl<sub>2</sub>O<sub>4</sub> is reduced, it is active for reforming reactions and is resistant to coking.

Wang and Lu<sup>175,176</sup> investigated the effect of various oxide supports in the catalytic performance and stability of Ni catalysts for dry reforming of methane. Results of their investigation are summarized in Table 6. Ni crystallites that formed on the SiO<sub>2</sub> surface were smaller in size, given the high surface area and well-developed porosity of these supports. Lower porosity of Ni/ $\alpha$ -Al<sub>2</sub>O<sub>3</sub> and Ni/TiO<sub>2</sub> resulted in lower dispersion of metal and, thus, in larger crystallite sizes. On the other hand, in spite of La<sub>2</sub>O<sub>3</sub> being nonporous, the Ni crystallites that formed on it were smaller in size. La<sub>2</sub>O<sub>3</sub> has a higher ability of dispersing metal particles on the surface. Regarding Ni catalysts supported on MgO, it is apparent that NiO–MgO catalysts form a solid phase. As a result, it is very hard to reduce the Ni in the Ni/MgO catalyst. It has to be prerduced at >800 °C to form active Ni crystallites.

#### 4. THERMODYNAMICS OF STEAM GASIFICATION OF BIOMASS

Biomass characteristics such as chemical and physical properties can vary widely as described in section 1. This variability may have a potential effect on gasification conditions and product quality. With this end in mind, thermodynamics can be a very useful engineering tool to assess how biomass composition, gasifier temperature, and pressure as well as steam-to-biomass ratio affect gasification.

Through thermodynamic analysis, one can determine the theoretical limits of the chemical species distributions at chemical equilibrium. Moreover, the thermodynamic efficiency, the available work of a given biomass fuel, and the optimum operating conditions can also be obtained by using this approach.<sup>179</sup> Thermodynamic results are in principle independent of the reaction network, type of the reactor, and/or reaction time.<sup>180</sup> However, in practice, thermodynamic predictions have inherent limitations, being suitable for gasification processes with long reaction times. This is the result of the role played by gasification kinetics under these conditions.<sup>181</sup>

#### 4.1. Nonstoichiometric Approach

At chemical equilibrium, a reacting system achieves a condition where the system entropy is maximized and the Gibbs free energy is minimized. Two approaches have been developed for equilibrium modeling: (a) stoichiometric and (b) nonstoichiometric. The “stoichiometric” approach requires a defined reaction incorporating all chemical species. In the “nonstoichiometric” formulation, on the other hand, no particular biomass chemical constituents are considered. The only input that must be specified is the feed elemental composition. This elemental C, O, H, S, and N composition can be readily obtained from ultimate analysis data. This method is particularly appropriate for reactions with uncertain mechanisms and feed streams like biomass whose precise chemical compositions are unknown. Although these nonstoichiometric-based models give satisfactory predictions of the H<sub>2</sub>/CO ratio and changes in chemical species with operating conditions, in most of the cases, the experimentally observed synthesis gas composition deviates from that of the expected equilibrium composition. Specifically, experimental methane composition, a very critical parameter that is used to define the heating value of the synthesis gas, deviates considerably from most of the model-predicted values. The main reasons for these deviation are due to the inadequate assumptions adopted such as (i) equilibrium conditions for some key reaction steps, (ii) char and tar considered as solid carbon, and (iii) ash treated as an inert species. To address these issues, a thermodynamic nonstoichiometric model was recently developed by CREC researchers<sup>19</sup> as reported in the upcoming sections.

#### 4.2. Thermodynamic Modeling of Biomass Gasification

Modeling of biomass steam gasification is a challenging task.<sup>34</sup> Biomass is different from coal and other carbonaceous feedstocks given its high level of volatiles (70–75%), its different physical and structural characteristics, and its various reactivities. In spite of this, there is still vast experience with coal and other carbonaceous feedstocks that can be used to advance future development in biomass gasification.

As stated in section 2, biomass gasification involves a complex combination of reactions in the solid and gas phases including pyrolysis, partial oxidation, and steam gasification. A summary of gasification reactions are given in Table 7. Pyrolysis is the thermal decomposition of the feedstock into gaseous, liquid, and solid products in the absence of an oxidizing agent. Partial oxidation processes use less than the stoichiometric amount of oxygen required for complete combustion. Steam reforming involves the reaction of water with the biomass-derived species to produce CO, CO<sub>2</sub>, and H<sub>2</sub>. The water gas shift (WGS) reaction

**Table 7. Chemical Reactions in the Steam Gasification of Biomass<sup>19</sup>**

name of reaction	chemical equation	$\Delta G_{f(298)}^{\circ}$ [kJ/mol]	$\Delta H_{f(298)}^{\circ}$ [kJ/mol]	$K_{(800 \text{ } ^\circ\text{C})}$
dry reforming of methane	$\text{CH}_4 + \text{CO}_2 \leftrightarrow 2\text{CO} + 2\text{H}_2$	168.635	123.760	132.013
steam reforming of methane	$\text{CH}_4 + \text{H}_2\text{O} \leftrightarrow \text{CO} + 3\text{H}_2$	140.098	205.310	169.182
water gas shift reaction	$\text{CO} + \text{H}_2\text{O} \leftrightarrow \text{H}_2 + \text{CO}_2$	-28.538	-42.200	1.0051
heterogeneous water gas shift reaction	$\text{C} + \text{H}_2\text{O} \leftrightarrow \text{H}_2 + \text{CO}$	89.824	130.414	7.0401
Boudouard equilibrium	$\text{C} + \text{CO}_2 \leftrightarrow 2\text{CO}$	118.362	172.615	6.499
hydrogenating gasification	$\text{C} + 2\text{H}_2 \leftrightarrow \text{CH}_4$	-50.273	-74.900	0.049
ethylene	$2\text{CO} + 4\text{H}_2 \leftrightarrow \text{C}_2\text{H}_4 + 2\text{H}_2\text{O}$	-111.651	-104.256	1.738e-08
ethane	$2\text{CO} + 5\text{H}_2 \leftrightarrow \text{C}_2\text{H}_6 + 2\text{H}_2\text{O}$	-212.787	-172.779	1.475e-08
propane	$3\text{CO} + 7\text{H}_2 \leftrightarrow \text{C}_3\text{H}_8 + 3\text{H}_2\text{O}$	-293.149	-165.051	8.743e-14
butane	$4\text{CO} + 9\text{H}_2 \leftrightarrow \text{C}_4\text{H}_{10} + 4\text{H}_2\text{O}$	-376.793	-161.968	7.669e-19
pentane	$5\text{CO} + 11\text{H}_2 \leftrightarrow \text{C}_5\text{H}_{12} + 5\text{H}_2\text{O}$	-457.916	-159.719	4.321e-24
hexane	$6\text{CO} + 13\text{H}_2 \leftrightarrow \text{C}_6\text{H}_{14} + 6\text{H}_2\text{O}$	-539.699	-158.303	2.785e-29

(water and CO react to form H<sub>2</sub> and CO<sub>2</sub>) and methanation (CO and H<sub>2</sub> react to form CH<sub>4</sub> and H<sub>2</sub>O) are two other important reactions that occur during gasification.<sup>86,93</sup>

Altafini and Mirandola<sup>182</sup> presented a coal gasification model using nonstoichiometric chemical equilibrium with minimization of the Gibbs free energy. These authors analyzed the influence of the biomass elemental composition and the gasifying agents/fuel ratio on the equilibrium temperature (adiabatic case) to obtain the gas product composition and the overall conversion efficiency. These authors concluded that this equilibrium model was also useful to calculate the products of the process. Ruggiero and Manfrida<sup>183</sup> emphasized the potential of the nonstoichiometric equilibrium models that consider the Gibbs free energy minimization.

Schuster et al.<sup>136</sup> developed a model for steam gasification of biomass by applying thermodynamic equilibrium calculations. Biomass was represented with an elemental composition. Comparisons were made between the predictions of the equilibrium model applied to steam gasification and the experimental results from Schuster et al.<sup>136</sup> and Rapagna et al.<sup>184</sup> Boissonnet et al.<sup>12,185</sup> stated that this model gives correct orders of magnitude and trends. However, these equilibrium models always overestimated the yields of H<sub>2</sub> and CO whereas they underestimated the yield of CO<sub>2</sub>. In addition, these equilibrium models predicted a gas nearly free of CH<sub>4</sub> and free of tars. These authors reported that solid carbon and CH<sub>4</sub> content were underestimated. Deviations were assigned to the relatively slow gasification and decomposition of CH<sub>4</sub>.

Ginsburg and de Lasa<sup>51</sup> modified a previously reported nonstoichiometric equilibrium model to analyze experimental data. Major product species such as H<sub>2</sub>, CO, CO<sub>2</sub>, H<sub>2</sub>O, and CH<sub>4</sub> were considered for equilibrium calculations. This model considered two main reactions in the gas phase at equilibrium: (a) steam reforming of methane and (b) water gas shift. The experimental product gas composition deviated from the equilibrium. This deviation was assigned to the inadequate assumption that the methane dry reforming reaction reaches equilibrium over the reaction times studied. On this basis, Ginsburg and de Lasa<sup>51</sup> concluded that a more comprehensive kinetic model for dry reforming of methane is required.

Mahishi and Goswami<sup>120</sup> and Mevissen et al.<sup>109</sup> used the software packages Stanjan and HSC-Chemistry, respectively, to

determine the composition of the synthesis gas at thermodynamic equilibrium. These calculations were developed on the basis of the classical Gibbs energy minimization approach. The calculated values were compared with experimental data and showed important deviations.

Kersten et al.<sup>186</sup> developed a quasi-equilibrium temperature model (QET). Calculations were made at temperatures lower than that of the typical gasifier. Kersten et al.,<sup>186</sup> Li et al.,<sup>127</sup> and Jand et al.<sup>187</sup> considered additional empirical relations together with thermodynamics to calculate the carbon conversion and the yield of CH<sub>4</sub>. These empirical-theoretical models provide good predictions, although they have limited applicability to the specific gasifiers under study. Whether extrapolations of these predictions to other gasifiers can be made is rather uncertain.

Li et al.<sup>127</sup> adapted a phenomenological-based nonstoichiometric chemical equilibrium model. These authors incorporated into it data from a circulating fluidized-bed gasifier. Unconverted carbon and formed methane data were used to define nonequilibrium factors. This model allowed for predicting product gas compositions, heating value, and cold gas efficiency.

Melgar et al.<sup>188</sup> proposed a mathematical model that combined chemical equilibrium and thermal balance in a downdraft biomass gasifier. According to the authors, this model helps to predict the behavior of different biomasses and is a potentially useful tool for optimizing the design and operation of downdraft biomass gasifiers.

Although most of the nonstoichiometric models analyzed in the technical literature consider gasification under atmospheric pressure, Srinivas et al.<sup>189</sup> examined a pressurized gasifier. This gasifier operates with compressed air and steam injection. According to this thermodynamic-based analysis, there is a moderate effect of gasifier pressure on gas composition. As a result, it is expected that gasifier pressure affects the heating value of the syngas produced, its temperature, and the exergy gasifier efficiency.

#### 4.3. CREC Thermodynamic Biomass Gasification Model

To address the various issues discussed in the previous section, a nonstoichiometric thermodynamic equilibrium model based on the elemental C, H, and O biomass composition was recently

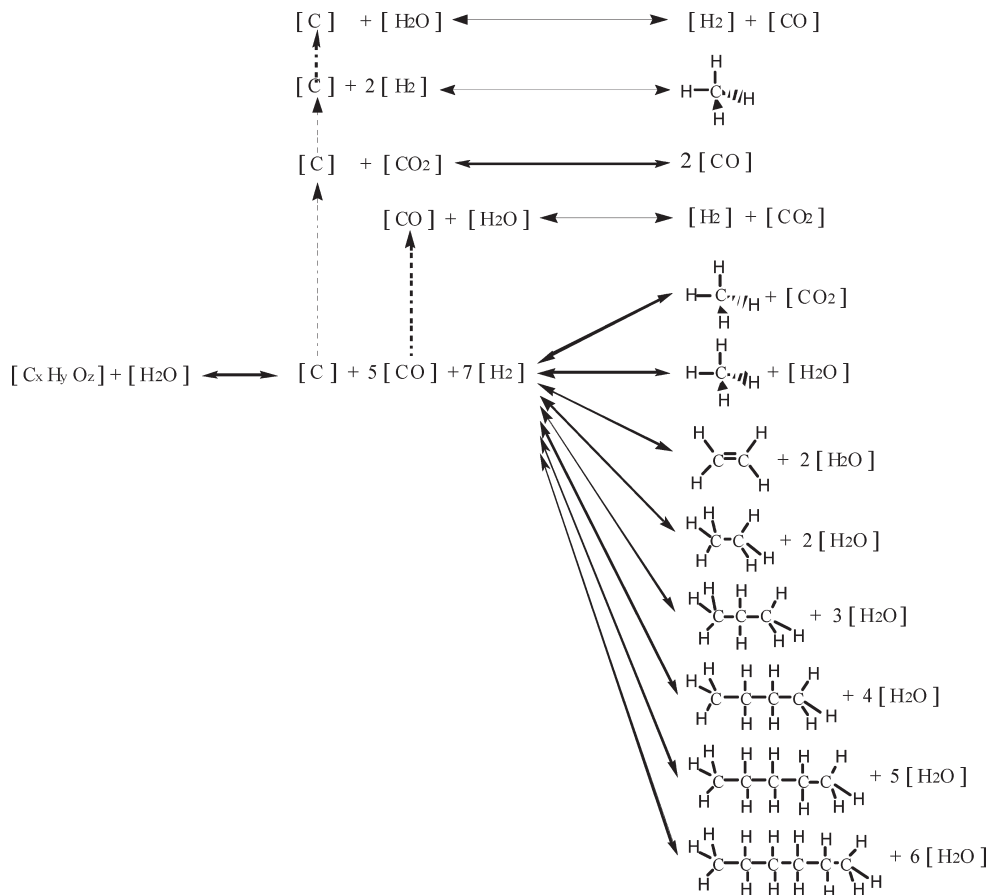
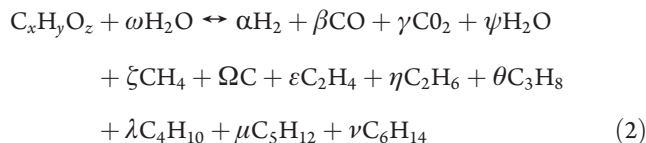


**Figure 8.** Chemical reaction network considered in the steam gasification of biomass as per Salaices et al.<sup>19</sup>

proposed by Salaices et al.<sup>19</sup> On this basis, the effects of fuel composition, temperature, pressure, and the amount of gasification agent were studied using Gibbs energy minimization.

The product species considered for equilibrium calculations were H<sub>2</sub>, CO, CO<sub>2</sub>, H<sub>2</sub>O, CH<sub>4</sub>, C<sub>2</sub>H<sub>6</sub>, C<sub>3</sub>H<sub>8</sub>, C<sub>4</sub>H<sub>10</sub>, C<sub>5</sub>H<sub>12</sub>, C<sub>6</sub>H<sub>14</sub>, and solid carbon.

From the elemental analysis of different biomasses, it can be proven that the contribution of nitrogen and sulfur species evolving from the reactor are negligible in terms of the equilibrium calculations.<sup>51,136</sup> Regarding tar, its formation was neglected given its low concentration. Thus, the simplified overall mass balance for the gasification reaction can be described as follows:



This proposed equilibrium model considered the main gas phase reactions described in Table 7 at equilibrium and which took place after the volatilization of biomass completed.

Nine independent nonlinear equations with nine unknowns result from the algebraic manipulation of this system of twelve variables ( $\alpha, \beta, \gamma, \psi, \zeta, \Omega, \varepsilon, \eta, \theta, \lambda, \mu, \nu$ ). The Newton–Raphson model is used to solve the nonlinear system of equations containing constrained variables. The Newton–Raphson method uses a truncated Taylor series estimate of the function values to obtain

better estimates of the unknowns. Additionally, a numerical solution of a subset of these equations was carried out successfully using Aspen HYSYS package for calculation verifications.

**4.3.1. Equilibrium Constants.** *4.3.1.1. Effect of Temperature on the Equilibrium Constant.* The standard property changes of reaction variables, such as  $\Delta G^\circ$  and  $\Delta H^\circ$ , vary with the equilibrium temperature as follows:<sup>190</sup>

$$\frac{d\Delta G^\circ}{dT} = -\ln K \quad (3)$$

and

$$\frac{d\ln K}{dT} = \frac{-\Delta H^\circ}{RT^2} \quad (4)$$

Equation 4 establishes the effect of temperature on the equilibrium constant and, hence, on the equilibrium conversion.

*4.3.1.2. Effect of Pressure on the Equilibrium Constants.* At reaction equilibrium, the gas species compositions are a function of both temperature and pressure. A description of the gas-phase composition can be made by applying Le Chatelier's principle to the reaction network as follows:

$$\frac{K}{[\Pi_i(\phi_i)^{v_i}]} = \left[ \frac{(y_{A3})^{v_3}(y_{A4})^{v_4}}{(y_{A1})^{v_1}(y_{A2})^{v_2}} \right] P^\nu \quad (5)$$

**4.3.2. Distribution of Product Species.** The influence of different biomass compositions on the product gas constituents

was examined by Salaices et al.<sup>19</sup> by varying, on one hand, the carbon-to-hydrogen content (in wt %, maf) and, on the other hand, the carbon-to-oxygen content. This variation was done over a wide range of fuel compositions: from carbon-to-hydrogen content of 1:2.11 (jute stick) to carbon-to-hydrogen content of 1:0.69 (coal), and carbon-to-oxygen content of 1:1 (glucose) to carbon-to-oxygen content of 1:0.111 (heterotrophic). To obtain results that could be compared, the temperature and pressure was set constant at 800 °C and 1 atm, respectively.

Figure 9 reports that the H<sub>2</sub> mole fraction of the product gas is a function of steam/biomass ratio for different biomass compositions. The hydrogen concentration in the product gas is shown

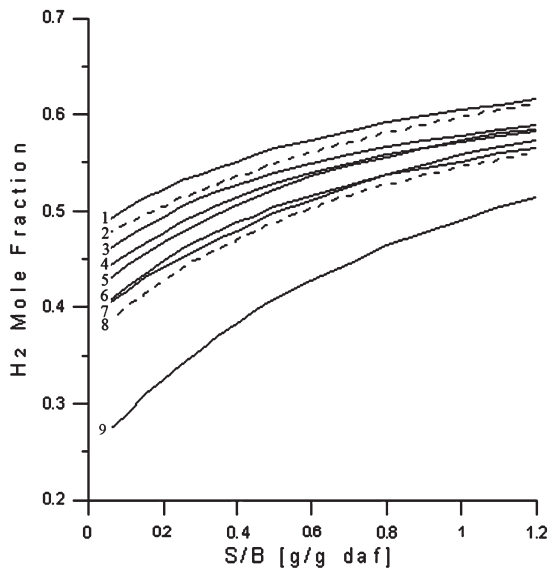


**Figure 9.** Hydrogen mole fraction versus steam/biomass ratio at 800 °C and 1 atm. Equilibrium model predictions of different biomass compositions. From higher to lower H<sub>2</sub> mole fraction: (1) jute stick, (2) glucose, (3) heterotrophic, (4) potato starch, (5) pine sawdust, (6) legume straw, (7) softwood bark, (8) wasted wood, and (9) coal.<sup>19</sup>

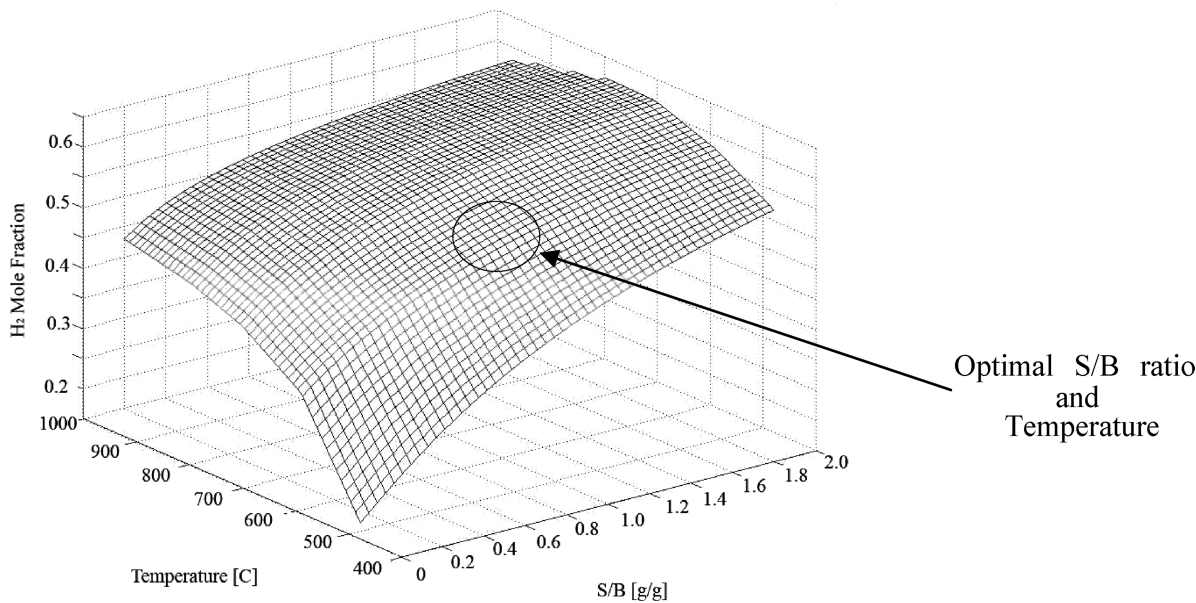
both to augment with increasing steam/biomass ratio from 0.0 to 2.0 and to be proportional with the carbon-to-hydrogen content in the biomass considered. This value is consistent with experimental data, as discussed in section 2.1 of this review. It is predicted that increasing the steam/biomass ratio beyond 1.0 g/g leads to a significantly higher concentration of H<sub>2</sub> in the product gas.

Figure 10 reports the predicted molar fractions of H<sub>2</sub> and their changes with temperature and S/B ratios.

Parts a–d of Figure 11 report the predicted H<sub>2</sub>, CO, CO<sub>2</sub>, CH<sub>4</sub>, and H<sub>2</sub>O product fractions and their changes with temperature at S/B of 0.1, 0.5, 1.0, and 1.5 g/g, respectively. One can see that the distribution of hydrogen is augmented with the increase in the steam/biomass ratio from 0.1 to 0.8. For steam/biomass ratios higher than 0.8, H<sub>2</sub> reaches a plateau at 800 °C (0.38 at S/B = 1.0 and 0.33 at S/B = 1.5), decreasing slightly after this temperature. On this basis, a steam/biomass ratio of 0.5–0.7 g/g and temperatures close to 800 °C were identified as optimal conditions for the process. It is at these conditions that the equilibrium model predicts the highest H<sub>2</sub>/CO ratio of 2.

Sensitivity analysis with this model shows that carbon-to-hydrogen content, gasification temperature, and steam/biomass ratio are the most significant parameters determining the chemical efficiency of steam gasification. Furthermore, thermodynamic equilibrium results were compared with experimental data at different reaction times. This was done to understand the relationship between thermodynamic predictions and chemical kinetics. Figures 12–15 report the molar fraction compositions of the major product species including H<sub>2</sub>, CO, CO<sub>2</sub>, and CH<sub>4</sub> as a function of steam/biomass ratio for (a) equilibrium model predictions, (b) catalytic steam gasification using a 2.5% Ni-supported catalyst at 5, 10, 20, and 30 s, and (c) noncatalytic steam gasification runs.<sup>19</sup>

Gasification runs, at various contact times, in de Lasa's CREC riser simulator<sup>191</sup> were reported by Salaices et al.<sup>19</sup> This reactor is a bench-scale internal recycle batch reactor with a capacity of 53 cm<sup>3</sup>, which allows for the loading of 1 g of catalyst. A series of sampling valves (Figure 16) complete the assembly of the CREC



**Figure 10.** Equilibrium fractional distribution of H<sub>2</sub> on a dry basis at P = 1 atm and various Steam/Glucose (S/B) ratios and Temperatures.<sup>19</sup>

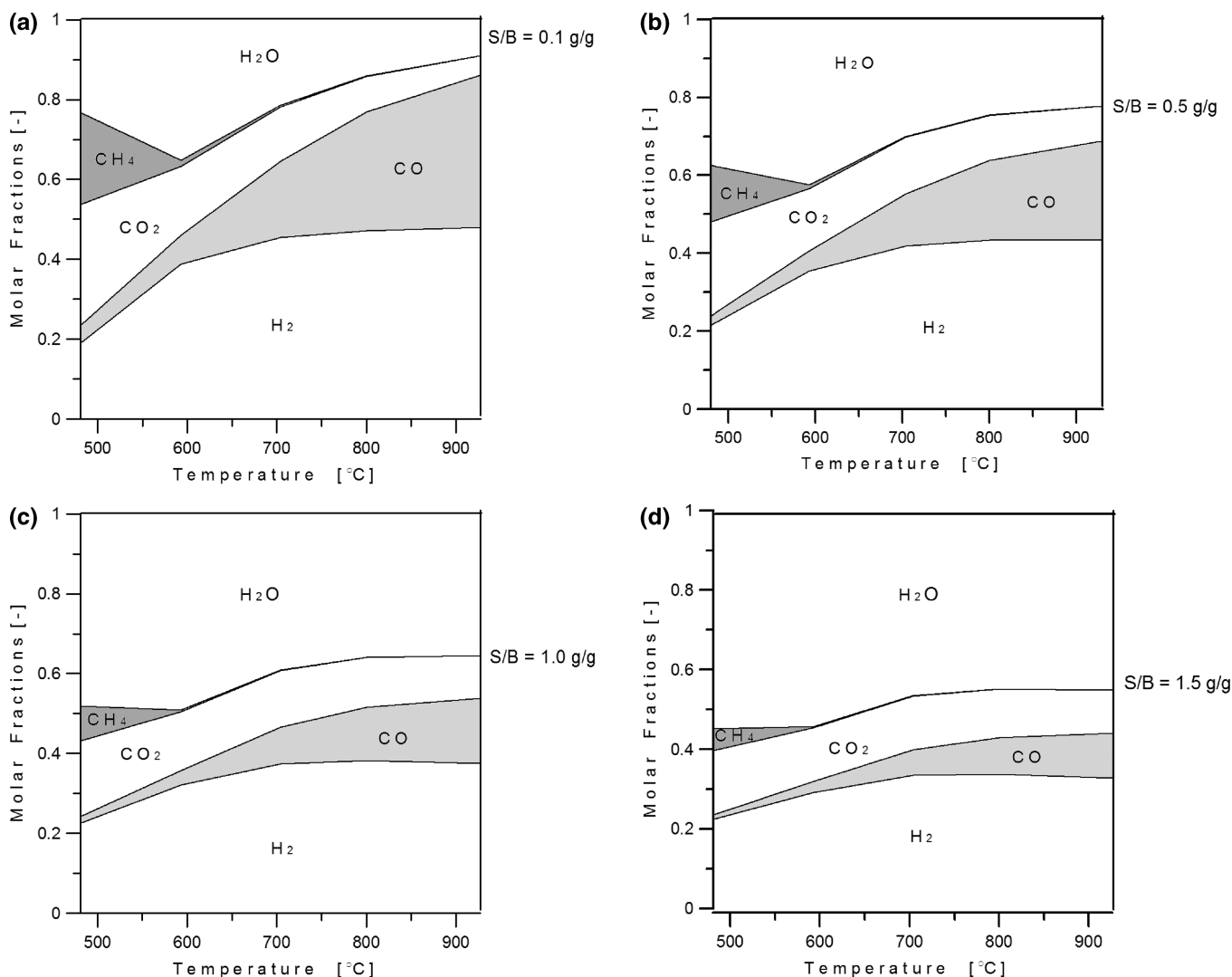


**Figure 11.** (a) Equilibrium fractional distribution of  $\text{H}_2$ ,  $\text{CO}$ ,  $\text{CO}_2$ ,  $\text{CH}_4$ , and  $\text{H}_2\text{O}$  at  $P = 1 \text{ atm}$ ,  $\text{S/B} = 0.1$ , and various temperatures.<sup>19</sup> (b) Equilibrium fractional distribution of  $\text{H}_2$ ,  $\text{CO}$ ,  $\text{CO}_2$ ,  $\text{CH}_4$ , and  $\text{H}_2\text{O}$  at  $P = 1 \text{ atm}$ ,  $\text{S/B} = 0.5$ , and various temperatures.<sup>19</sup> (c) Equilibrium fractional distribution of  $\text{H}_2$ ,  $\text{CO}$ ,  $\text{CO}_2$ ,  $\text{CH}_4$ , and  $\text{H}_2\text{O}$  at  $P = 1 \text{ atm}$ ,  $\text{S/B} = 1.0$ , and various temperatures.<sup>19</sup> (d) Equilibrium fractional distribution of  $\text{H}_2$ ,  $\text{CO}$ ,  $\text{CO}_2$ ,  $\text{CH}_4$ , and  $\text{H}_2\text{O}$  at  $P = 1 \text{ atm}$ ,  $\text{S/B} = 1.5$ , and various temperatures.<sup>19</sup>

riser simulator and allow the withdrawal of chemical species in short periods of time. In addition, a gas chromatographic unit allows the analysis of reaction products using thermal conductivity, flame ionization, and mass spectrometric detectors.

Considering the experimental results obtained,<sup>19</sup> it becomes apparent that the water gas shift, the reforming of methane, and higher hydrocarbons reactions do not reach thermodynamic equilibrium over short reaction times (5–30 s). Therefore, although the equilibrium model satisfactorily predicts trends for all individual species in the product gas for longer reaction times (>30 s), it was observed in experiments that product gas compositions deviate from the equilibrium model at the shorter reaction times (<10 s). These results prove that gasification products are not in equilibrium at contact times smaller than 10 s and that a nonequilibrium model is needed to fully describe the interconversion of gaseous species in biomass steam gasification.

Exergy analysis allows us to evaluate quantitatively the energy losses that occur in thermal and chemical processes.<sup>192</sup> Thus, having the product gas composition exiting the gasifier as well as

the exergy efficiency allows one to rank the efficiency of different biomass gasification technologies. Toonssen et al.<sup>193</sup> compared different commercial or pilot-scale gasification systems for the design of a hydrogen production plant. The processes were compared on the basis of thermodynamic performance (hydrogen yield and exergy efficiency).

#### 4.4. Thermodynamic Analysis of Coke Formation

Coke formation is an important phenomenon in the biomass gasification process that requires special attention and thermodynamic analysis. However, to our knowledge, only one published article deals with the thermodynamic model to explain the formation of coke under dry reforming conditions. Interested readers can consult Ginsburg and de Lasa.<sup>51</sup> The decomposition of methane ( $\text{CH}_4 \rightarrow \text{C} + 2\text{H}_2$ ) and the disproportionation of carbon monoxide ( $2\text{CO} \rightarrow \text{CO}_2 + \text{C}$ ) are two accepted modes of carbon deposition on the catalyst/support. The amount of coke deposited on the catalyst depends on the  $\text{CH}_4/\text{CO}_2$  feed ratio and the operating temperature and pressure.

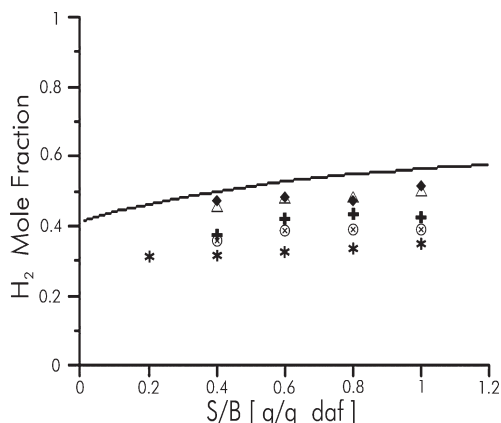


**Figure 12.** H<sub>2</sub> mole fractions of product gas for gasification of glucose at different steam/glucose ratios, 700 °C, and P = 1 atm. Solid line (—) equilibrium model, (\*) noncatalytic gasification runs, experimental data using 2.5% Ni supported catalyst at (○) 5, (+) 10, (△) 20, and (◆) 30 s of reaction time.<sup>19</sup>

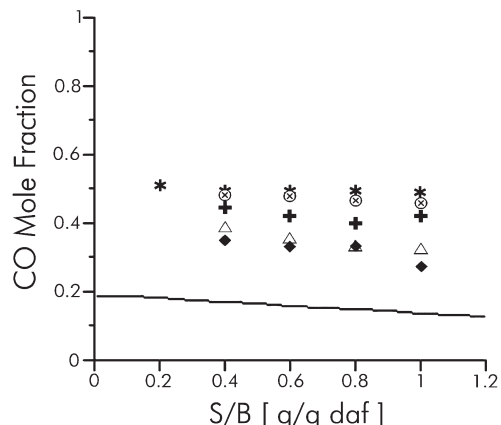


**Figure 13.** CO mole fractions of product gas for gasification of glucose at different steam/glucose ratios, 700 °C, and P = 1 atm. Solid line (—) equilibrium model, (\*) noncatalytic gasification runs, experimental data using 2.5% Ni-supported catalyst at (○) 5, (+) 10, (△) 20, and (◆) 30 s of reaction time.<sup>19</sup>

Methane decomposition (eq 6) is an endothermic reaction whereas carbon monoxide disproportionation (eq 7) is exothermic.



with  $K_i$  and  $\Delta G^\circ$  defined with eqs 3 and 4 as reported by Ginsburg and de Lasa.<sup>51</sup>

$$\alpha = \frac{p_{\text{H}_2}^2}{p_{\text{CH}_4} p_0} \text{ and } \beta = \frac{p_{\text{CO}_2} p_0}{p_{\text{CO}}^2} \quad (8)$$

It was postulated that if both  $\alpha > K_6$  and  $\beta > K_7$  then coke formation would be thermodynamically allowed.<sup>51</sup>

More recently, Salaices<sup>27</sup> postulated that to provide a proper assessment of carbon formation the  $\text{CO} + \text{H}_2 \leftrightarrow \text{C} + \text{H}_2\text{O}$  reaction should also be considered with  $\gamma > K_8$ : (a)  $K_i$  defined with eqs 3 and 4 and (b)  $\gamma = (p_{\text{H}_2\text{O}} p_0) / (p_{\text{CO}} p_{\text{H}_2})$ .

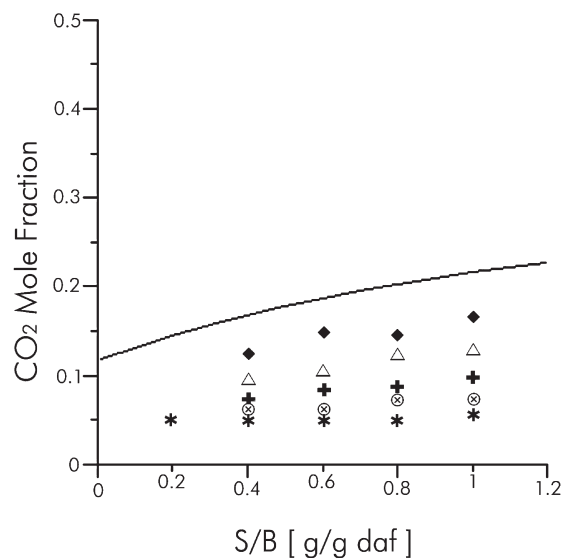


**Figure 14.** CO<sub>2</sub> mole fractions of product gas for gasification of glucose at different steam/glucose ratios, 700 °C, and P = 1 atm. Solid line (—) equilibrium model, (\*) noncatalytic gasification runs, experimental data using 2.5% Ni-supported catalyst at (○) 5, (+) 10, (△) 20, and (◆) 30 s of reaction time.<sup>19</sup>

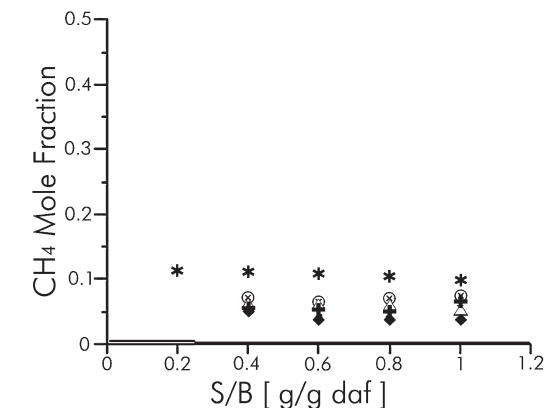


**Figure 15.** CH<sub>4</sub> mole fractions of product gas for gasification of glucose at different steam/glucose ratios, 700 °C, and P = 1 atm. Solid line (—) equilibrium model, (\*) noncatalytic gasification runs, experimental data using 2.5% Ni-supported catalyst at (○) 5, (+) 10, (△) 20, and (◆) 30 s of reaction time.<sup>19</sup>

Reported trends of experimental data show that both  $\alpha$  and  $\beta$  are  $\alpha < K_6$  and  $\beta < K_7$  for all reaction times. This shows that methane decomposition and the Boudouard reaction favor carbon formation. On the other hand, one can also notice that  $\gamma$  is consistently larger than  $K_8$  for the  $\text{CO} + \text{H}_2 \leftrightarrow \text{C} + \text{H}_2\text{O}$  reaction with this favoring carbon conversion. As a result, it can be assumed that there is a balance between coke formation (eqs 6 and 7) and coke removal reaction (reverse of  $\text{CO} + \text{H}_2 \leftrightarrow \text{C} + \text{H}_2\text{O}$ ). This yields, under these condition studies, a negligible amount of coke.<sup>27</sup>

#### 4.5. Gas-Phase Reactions: At Thermodynamic Equilibrium or Kinetically Limited?

The gas-phase chemical species are assumed to be constituted by H<sub>2</sub>, CO, CO<sub>2</sub>, CH<sub>4</sub>, and H<sub>2</sub>O. As already stated, the thermodynamic equilibrium models assume that reactants reach chemical equilibrium.<sup>194</sup> Salaices et al.<sup>19</sup> showed, for instance,

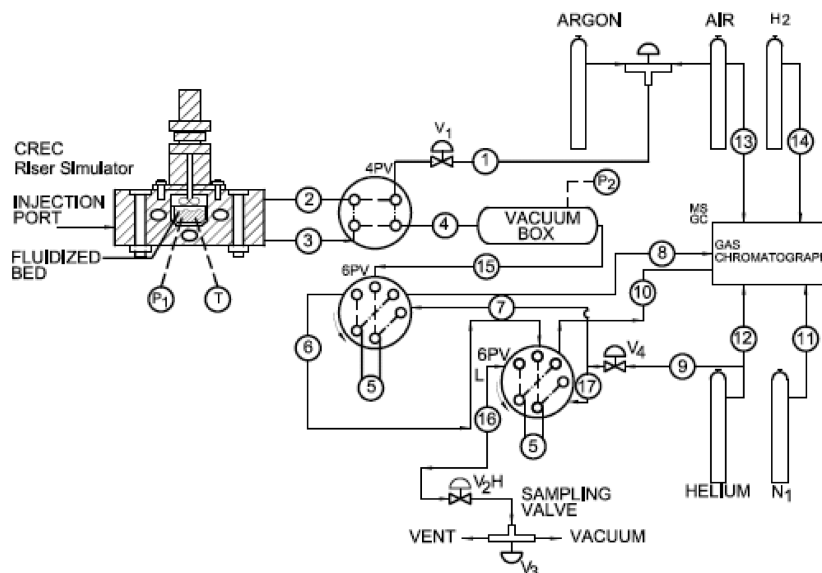


**Figure 16.** Schematic description of the CREC riser simulator and its accessories. 4PV: (i) 1–2–3–4 connected, reactor is evacuated; (ii) 2–3 connected, gasification experiment is taking place. 6PV: (i) 15–5–6 and 6–5–16 connected, sample is being loaded in sampling loops; (ii) 7–5–8 and 17–5–10 connected, sample is being carried to the GC for analysis. Adapted with permission from ref 27. Copyright 2010.

that the applicability of these chemical equilibrium hypotheses is strongly dependent on gasification time.

Rapagna et al.<sup>184</sup> compared calculated constants for the water gas shift reaction as in eq 9,

$$K_{WGS,exp} = \frac{P_{CO_2,exp} P_{H_2,exp}}{P_{CO,exp} P_{H_2O,exp}} \quad (9)$$

with the equilibrium constants for the water gas shift reaction resulting from thermodynamic equilibrium considerations.

As shown in Table 8, at 820 °C and at 1 bar of total pressure, the theoretically derived thermodynamic equilibrium constants deviate significantly from the eq 9 constant obtained from experimentally observed gas species compositions. These deviations can result from incomplete cracking of the pyrolysis products, temperature differences inside the gasifier, and/or catalytic effects. In fact, many steel alloys contain nickel, which can have a selective catalytic activity on methane pyrolysis kinetics.<sup>195</sup>

Furthermore, it is important to establish which one of the gas phase reactions considered is kinetically controlled. With this end, the steam reforming of CH<sub>4</sub> was studied using Chemkin software.<sup>136,196</sup> The calculated compositions are nearly constant from 100 to 1000 s and significantly different from the equilibrium compositions (Table 9). On this basis, it can be concluded that the steam reforming of CH<sub>4</sub> is a kinetically limited reaction step.

The experimental verifications of equilibrium conditions by Schuster et al.<sup>136</sup> and Rapagna et al.<sup>184</sup> were performed in biomass steam gasification fluidized beds. On the other hand, Zanzi<sup>197</sup> studied them in a biomass flash pyrolysis free-fall reactor. The results of these calculations are given in Table 10. In the experiments of Schuster et al.<sup>136</sup> and Rapagna et al.,<sup>184</sup> the calculated constants are of the same order of magnitude as the equilibrium constants. Under 800–1000 °C, 1 bar of total pressure, and 0.3–1.2 steam–biomass ratio, the water gas shift reaction can safely be assumed to be close to equilibrium. On the other hand, in the tests by Zanzi<sup>197</sup> developed at 800 °C, a difference of ~1 order of magnitude was observed between the experimental

**Table 8. Experimental Gas-Phase Composition and Equilibrium Constants for the Water Gas Shift Reaction; Prepared with Data from Rapagna et al.<sup>184</sup>**

mol/mol dry biomass input	experimental gas compositions <sup>184a</sup>	K <sub>WGS,exp</sub>	K <sub>WGS,eq</sub>
H <sub>2</sub>	34.2	0.87	0.95
CO	19.0		
CO <sub>2</sub>	13.3		
H <sub>2</sub> O	27.5		
CH <sub>4</sub>	6.0		

<sup>a</sup> Reaction conditions: T = 1093 K; p = 1 bar; steam/dry biomass = 0.7 kg/kg; olivine.

constants and the equilibrium constant. At 1000 °C, however, the chemical equilibrium conditions appear to have been attained.

It is relevant to note that several authors claim that water gas shift reaches equilibrium at 800 °C.<sup>108,198</sup> Schuster et al.<sup>136</sup> and Rapagna et al.<sup>184</sup> confirmed this assumption using an Fe catalyst. This catalyst promotes the water gas shift reaction. The presence of excess steam also favored the water gas shift reaction.

Thus, as a first approximation, it appears that, under typical operating gasification conditions of interest (800 °C < T < 1000 °C, P = 1 bar), it can be safely assumed that the water gas shift reaction is at equilibrium whereas the steam reforming of CH<sub>4</sub> is kinetically limited.

#### 4.6. Optimizing Gasifier Operating

Lower-temperature catalytic steam gasification of biomass is being investigated as an environmentally friendly alternative for hydrogen production. In this respect, Moghtaderi<sup>199</sup> found that a relatively low reaction temperature of 600 °C, a 20 min residence time, and a high steam content of ~90% is suitable for maximizing hydrogen production. In this respect, a thermodynamic model was very useful to research optimum conditions. Mahishi and Goswami<sup>120</sup> determined optimum operating conditions at

727 °C, a steam/biomass ratio of 3, and an ER of 0.1. It was observed that temperature increases favor hydrogen production, while higher temperatures yields a product gas with a slightly lower LHV. In addition, the temperature showed an important influence on tar removal. Increasing S/B ratio favored steam reforming and decreased total organic carbon (TOC) content.<sup>119</sup> Thus, to get optimum H<sub>2</sub> yields, with negligible CH<sub>4</sub> and coke formation, a best practice is to operate the gasifier at 627–827 °C. Moreover, pressure can be increased from 1 to 3 atm at a temperature above 827 °C, further increasing H<sub>2</sub> yields.<sup>200</sup>

CREC researchers<sup>19</sup> predicted that a steam/biomass ratio of 0.5–0.7 g/g and temperatures above 800 °C were best for maximizing the H<sub>2</sub> output without compromising the process energy efficiency. This is in agreement with the research group Franco et al.,<sup>50</sup> who found that the optimum operating gasifier conditions were at 830 °C with a steam/biomass ratio of 0.6–0.7 g/g.

Moreover, Wang et al.<sup>201</sup> reported, in this respect, that optimum conditions for hydrogen production were at temperatures 662–700 °C with water/glycerin ratios of 9–12 at atmospheric pressure. These authors indicated that temperatures above 762 °C, water/glycerin ratios of 2–3, and 20–50 atm were the preferred conditions for producing synthesis gas with a H<sub>2</sub>/CO ratio suitable for methanol production and for Fischer–Tropsch synthesis. It was expected that, under these optimum conditions, carbon formation could be thermodynamically inhibited.

## 5. KINETIC STUDIES OF CATALYTIC STEAM GASIFICATION OF BIOMASS

### 5.1. Kinetic Modeling

As already stated in section 4, the steam gasification of biomass is a complex network of heterogeneous reactions. One can envision

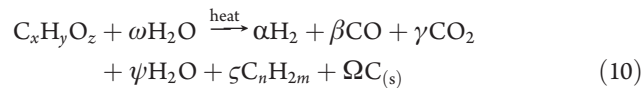
**Table 9. Simulation of the Evolution of the Experimental Gas-Phase Composition versus Time and Gas-Phase Composition at Equilibrium<sup>196</sup>**

	gas composition				
	(mol %)	0 s	100 s	1000 s	equilibrium
Dupont et al et al <sup>196</sup>	H <sub>2</sub>	33.2	33.2	33.4	42.0
T = 1093 K, p = 1 bar	CO	15.6	15.6	15.4	19.0
	CO <sub>2</sub>	14.4	14.4	14.6	12.6
	CH <sub>4</sub>	4.40	4.40	4.39	0.02
	H <sub>2</sub> O	32.4	32.4	32.2	26.4

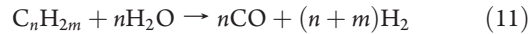
**Table 10. Experimental Constants and Equilibrium Constants of Water Gas Shift Reaction**

name of experiment	UNIVAQ 1 kW	FICFB 10 kW	Zanzi birch 3
source	Rapagna et al <sup>184</sup>	Schuster et al <sup>136</sup>	Zanzi <sup>197</sup>
reactor	Fluidized bed	Fluidized bed	Free-fall reactor
type of biomass	Almond shells	Wood	Birch wood
	C <sub>6</sub> H <sub>8.6</sub> O <sub>3.7</sub>	C <sub>6</sub> H <sub>8.8</sub> O <sub>3.6</sub>	C <sub>6</sub> H <sub>8.3</sub> O <sub>4.2</sub>
particle size (mm)	1.1	not given	0.8–1
T (K)	1093	1123	1273
steam/dry biomass (kg/kg)	1.2	0.3	0
bed materials	olivine	sand	no catalyst
gas residence time	not given	not given	~3 s
solid residence time	not given	not given	~1 s
experimental constant K <sub>shift exp</sub>	0.9	0.9	0.7
equilibrium constant K <sub>shift eq</sub>	1.0	0.9	0.6
K <sub>shift exp</sub> /K <sub>shift eq</sub>	0.9	1	1.2

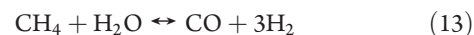
biomass gasification as a combination of primary and secondary reactions. Primary reactions break down the vaporized biomass molecules, forming coke and permanent gases:



Secondary reactions crack the higher hydrocarbons into gases that further combust or become reduced:



Furthermore, permanent gases react to alter the gas composition depending on gasifier conditions as indicated below:



One can also provide a description of steam gasification on the basis of a single overall stoichiometry where chemical species are grouped in “lumps” (char, gases, and tar):



### 5.2. Time Scale Analysis

To address kinetic modeling, an adequate starting point is the definition and comparison of the time scales, associated with the different physicochemical phenomena involved. The time scale analysis has been mainly used in the case of pyrolysis.

In this respect, Pyle and Zaror<sup>202</sup> studied particle external heat transfer limitations. Experimental data were used to validate the simplified models for different particle sizes under slow pyrolysis conditions. Furthermore, Bryden et al.<sup>203</sup> considered the cases in which both internal and external heat transfer processes were limiting.

However, and in order for an overall gasification process to be controlled by intrinsic kinetics, a maximum particle size has to be defined at various operating temperatures. Simmons and Gentry<sup>204</sup> defined, in this respect, the boundaries between thermal and chemical regimes as a function of temperature and particle size. The potential influence of heat transfer on biomass was also shown at different gas velocities. At 500 °C, and according to their calculations, the particles sizes smaller than 100 μm are gasified in the chemically controlled regime. Nevertheless, according to the various pyrolysis experiments developed by these authors, biomass particle sizes have to be further reduced to 10 μm to achieve a chemically controlled kinetic condition.

More recently, Peters and Bruch<sup>205</sup> plotted the ratio of characteristic times for intrinsic chemical reactions and internal heat conduction time, versus the particle diameter. These authors developed this calculation for different temperatures up to 600 °C. It was found that, at this temperature, the transition zone between the chemical and thermal regimes takes place between 50 and 500 μm.

One can note that boundaries between regimes resulting from the time scale analysis developed by Peters and Bruch<sup>205</sup> and Simmons and Gentry<sup>204</sup> are not in good agreement. These differences may be due to discrepancies in the experimental data used and to different operating conditions considered, namely, the heating rates.

Thus, the characteristic time analysis provides an effective way to establish simplified models with physical meaning. Nevertheless, such simplified models are restricted in their application to the specific range of operating conditions studied.

### 5.3. Kinetic Models at Particle Scale

Sophisticated models have been derived for biomass gasification, taking the physicochemical changes occurring at the particle scale as the main determining events. These are the following:

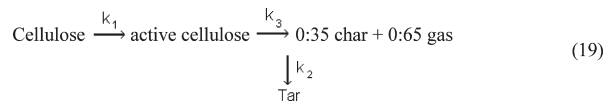
- Pyrolysis, which accounts for the decomposition of the initial solid biomass into permanent gases, condensable gases called tars, and a solid residue called char.
- Gasification, which considers the reaction of the solid residue with reactive gases such as steam.

Models are based on mass and energy balances over the particle, as well as the associated boundary conditions. Differences between models are caused by the difference in physical properties of the biomass particles during gasification and their evolution with time or conversion. Detailed accounting of these properties and their evolution sometimes may dramatically increase the number of model adjustable parameters.

Concerning the chemistry of steam gasification of biomass residue, most authors assume that the solid residue is pure carbon. Kinetic laws obtained on coal or pure carbon are then used.<sup>206,207</sup> Note that Di Blasi<sup>208</sup> approximately accounts for the true nature of biomass by considering the amount of H and O in the residue. Matsui et al.<sup>209</sup> described the heterogeneous reaction of carbon with steam and the water gas shift in a single reaction, with a  $(1 + \beta)$  stoichiometric coefficient associated to  $\text{H}_2\text{O}$ . From a thermodynamic or kinetic viewpoint, lumping together two independent reactions is risky and should be avoided, especially when one of these reactions, namely, the water gas shift, may not be close to equilibrium.

For the description of the pyrolysis chemistry, semiglobal mechanisms are proposed, which are given in ref 19. These descriptions are interesting because they seem to be a first step

toward understanding the complex chemistry of pyrolysis. Nevertheless, the composition of the gases produced cannot be predicted by this model. One possible cause is the lack of adequate consideration of the solid C, H, and O elemental compositions as input data in this model. In this respect, the biomass to be gasified is considered as a single pseudospecies, such as biomass or wood, or as a mixture of species.<sup>210</sup>



Although significant efforts have been made in the description of different transport processes involved in biomass gasification, models still describe the complex chemical phenomena poorly. Contrary to physical phenomena, there is limited ability to describe intrinsic gasification rates and the nature of the chemical pathways. These various pathways can also vary in importance with the operating conditions, especially with changes in the heating rates. Additionally, more detailed descriptions of chemical pathways augment the number of model parameters to be determined. Parameter reliability, confidence intervals, and consistency of the derived kinetics are rarely discussed.

### 5.4. Intrinsic Kinetics for Biomass Gasification: The CREC "Additive Effect" Model

As stated above, one possible approach toward successful gasification kinetic modeling is the use of biomass particles of a small enough size to ensure that the intrinsic kinetic is the controlling step. Another useful strategy is to use biomass surrogates such as glucose and/or phenolic species that allow the simulation of the main components of biomass (e.g., cellulose and lignin).<sup>19</sup>

Lv et al.<sup>211</sup> proposed a kinetic model of biomass catalytic pyrolysis, in which the entire process is treated as a single reaction. It assumes that biomass first decomposes to gaseous products, tars, and chars via three competitive reactions. Tars undergo a second cracking reaction producing gases and chars. Through the proposed model, the calculated data fit well with the experimental data obtained from pyrolysis tests of pine sawdust, lignin, and cellulose. The calculated reaction order is in the range of  $n = 0.66 - 1.57$ .

Radmanesh et al.<sup>212</sup> developed a biomass gasification model in a bubbling fluidized-bed reactor. The reactor model takes into account the pyrolysis and the heterogeneous and homogeneous reaction kinetics, as well as the hydrodynamics of the bed and freeboard. The two-phase model with nonadjustable parameters was used to describe the gas phase in the bed, and a counter-current back-mixing zone was considered for char mixing. It was shown that pyrolysis is an important step that can be a determining factor in the resulting product distribution and thus in the heating value of the produced fuel gas. This model also showed agreement with experiments in wood steam gasification.

Corella and Sanz<sup>213</sup> presented a one-dimensional semiempirical model for an atmospheric circulating fluidized-bed biomass gasifier. The kinetic equations for a proposed reaction network are solved together with mass and heat reactor balances and several fluid dynamic considerations. On this basis, the axial concentration profiles of ten different species and the bed temperature were calculated.

Fiaschi and Michelini<sup>212</sup> developed biomass gasification kinetics in a bubbling fluidized bed. This is a one-dimensional model that is able to predict temperature and concentration

gradients along the reactor axis. This model considers two phases, a bubble phase and a dense phase. Mass transfer between the two phases and a quantitative estimation of local bubble properties and particle properties is accounted for. A relatively simple reaction kinetics is incorporated in the dense phase. These authors claimed that the proposed kinetics showed substantial agreement with experimental data from the literature and with available gasification kinetics.

One can draw the conclusion that kinetic models consider subsets of reactions under a wide range of gasification conditions. In general, studies consider (i) the kinetically limited steam reforming of methane and (ii) the close to equilibrium water gas shift reaction.<sup>51,126,136,183,184,214</sup>

However, one can see that one of the main shortcomings of the proposed gasification kinetic models is that they lump together a complex network of heterogeneous reactions into one single kinetic rate equation. Although this, in principle, circumvents a model with too many parameters (overparameterization), the resulting rate equation provides an empirical fitting only. These kinetic models have little or no connection with the phenomenological events of either species adsorption or catalytic reaction taking place.

Salaices et al.<sup>215</sup> were the first ones to overcome this dilemma by demonstrating the viability of establishing, as is demonstrated in the upcoming sections, kinetic models using a sound reaction engineering approach. Reaction rates for various species were expressed as the algebraic addition (“additive effect”) of the dominant reactions as follows:

$$r_i = \nu_{WGS,i} \frac{r'_{WGS,r}}{\nu_{WGS,r}} + \nu_{SR,i} \frac{r'_{SR,r}}{\nu_{SR,r}} + \nu_{DRM,i} \frac{r'_{DR,r}}{\nu_{DR,r}} \quad (20)$$

where

$$r'_{WGS,H_2} = \frac{k'_{WGS} p_{CO} p_{H_2O}}{1 + 2K_{CO_2}^A p_{CO_2}} \left( 1 - \frac{p_{H_2} p_{CO_2}}{K_{WGS} p_{CO} p_{H_2O}} \right) \quad (21)$$

$$r'_{SR,CO} = \frac{k'_{SR} p_{CH_4} p_{H_2O}}{1 + 4K_{CH_4}^A p_{CH_4}} \left( 1 - \frac{p_{CO} p_{H_2}^3}{K_{SR} p_{CH_4} p_{H_2O}} \right) \quad (22)$$

$$r'_{DRM,CH_4} = -\frac{k'_{DRM} p_{CO_2} p_{CH_4}}{1 + 4K_{CO_2}^A p_{CO_2}} \left( 1 - \frac{p_{CO}^2 p_{H_2}^2}{K_{DRM} p_{CO_2} p_{CH_4}} \right) \quad (23)$$

It can be noted that each of these equations include phenomenologically relevant intrinsic kinetic parameters, such as  $k'$ , and adsorption constants,  $K_j^A$ .

One of the highlights of this approach is the kinetic model development in the CREC riser simulator. Adsorption and intrinsic kinetic parameters in this unit can be determined independently (*decoupled*).<sup>27</sup> As a result, the CREC riser simulator allows one to obtain data that can be used either for adsorption or reaction, with each of these cases having a limited number of parameters. As reported in Table 11, this limited number of phenomenologically relevant parameters was established with their parameter statistical indicators (spans for the 95% confidence interval and low cross-correlation).<sup>215</sup>

Table 11 reports the pre-exponential factor and energies of activation for the gasification of glucose in water at S/B ratios of 0.4, 0.6, 0.8, and 1.0, as a function of the reaction temperature. The proposed kinetic model provides sound energies of

**Table 11. Intrinsic Kinetic Parameters of the Proposed “Additive” Kinetic Model with Their 95% Confidence Interval<sup>215</sup>**

parameter	value	span for 95% confidence
$k'_{WGS}^a$	$3.7 \times 10^{-6}$	$\pm 3.1 \times 10^{-7}$
$E_{WGS}^b$	46.7	$\pm 1.6$
$k'_{SR}^c$	$2.0 \times 10^{-9}$	$\pm 5.8 \times 10^{-10}$
$E_{SR}^b$	96.3	$\pm 6.7$
$k'_{DRM}^c$	$3.8 \times 10^{-9}$	$\pm 3.3 \times 10^{-10}$
$E_{DRM}^b$	73.7	$\pm 0.9$
$K_{CO_2}^d$	$8.4 \times 10^{-2}$	$\pm 1.9 \times 10^{-3}$
$\Delta H_{CO_2}^A$	-11.01	$\pm 6.1$
$\sigma^e$	$1.5 \times 10^{-3}$	
$m$	240	

<sup>a</sup> [mol gcat<sup>-1</sup> s<sup>-1</sup> psia<sup>-1</sup>]. <sup>b</sup> [kJ/mol]. <sup>c</sup> [mol gcat<sup>-1</sup> s<sup>-1</sup>]. <sup>d</sup> [psia<sup>-1</sup>]. <sup>e</sup>  $\sigma = (\sum(X_{\text{experimental}} - X_{\text{estimated}})^2)^{1/2}/(m - p)$ , where  $m$  is the number of data points and  $p$  is the number of model parameters.

activation in the case of the cellulose surrogate (e.g., glucose) for the WGS, dry reforming of methane (DRM), and steam reforming of methane (SRM) reactions.<sup>27</sup> Similar encouraging findings were obtained for 2-methoxy-4-methylphenol, a lignin surrogate.<sup>27</sup> It can thus be concluded that the proposed model has great prospects for the prediction of biomass gasification in large-scale circulating fluidized-bed units.

## 6. CONCLUSIONS AND FUTURE PROSPECTS

- There is a great interest to develop and commercialize new catalysts for making biomass steam gasification in fluidized beds a viable option.
- Disposable catalysts for steam biomass gasification such as dolomite and olivine are a possible alternative. These naturally occurring materials have attracted much attention because they are cheap and disposable. The main issue with them is that they are not specifically manufactured for the challenging conditions of fluidized beds: Fluidization may be poor and attrition may be high, as is the case of dolomite.
- Biomass steam gasification using synthetic catalysts is also a most valuable option with great potential. In particular, nickel-based catalysts with adequate fluidizable supports and/or with the addition of dopants appear to open excellent possibilities for catalytic biomass gasifiers. These nickel-based catalysts can be specifically engineered to have the desired catalytic functions and the physical properties for low attrition and good fluidization.
- Thermodynamic analysis provides a valuable tool for assessing the effect of various operating conditions in biomass gasifiers.
- Thermodynamic models help identify operating conditions leading to high hydrogen yields or to a synthesis gas of high H<sub>2</sub>/CO ratio, such as the one required for methanol synthesis.
- Thermodynamic models present limitations in terms of their applicability for biomass residence times smaller than 20 s.

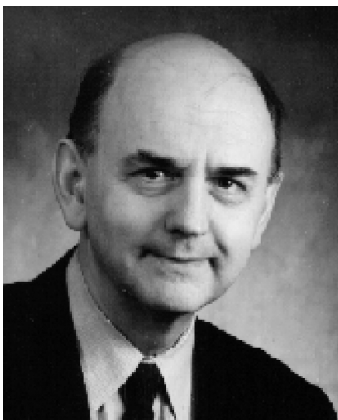
- (g) Thermodynamic models are adequate as shown by the CREC—UWO research group for biomass residence times larger than 30 s.
- (h) The time scale kinetic analysis and the particle-scale models provide valuable insights into the potential influence of the transport processes in biomass gasification. These models also provide guidelines on desirable biomass particle size for gasification processes controlled by chemical kinetics.
- (i) The establishment of intrinsic kinetic models for steam gasification of biomass requires new approaches. One good example is the Salaices et al model,<sup>19</sup> where the main gasification reactions are all included as an algebraic addition of chemical reaction events.
- (j) The evaluation of kinetic parameters requires new experimental strategies, as is the case of the one proposed in the CREC riser simulator. Evaluation of intrinsic kinetic parameters and adsorption constants are *decoupled* in their assessment, eliminating overparameterization. This also yields phenomenologically based parameters that can be linked to intrinsic reaction kinetics and used for effective scale-up of biomass gasifier units.

## AUTHOR INFORMATION

### Corresponding Author

\*E-mail: hdelasa@eng.uwo.ca. Phone: (519) 661-2144. Fax: (519) 850-2931.

## BIOGRAPHIES



Hugo I. de Lasa is a Professor at the Department of Chemical and Biochemical Engineering, Faculty of Engineering of the University of Western Ontario. He is the founding Director of the University of Western Ontario's Chemical Reactor Engineering Centre (CREC). In 1998, Hugo de Lasa received the Research Excellence Prize from the Faculty of Engineering Science of the University of Western Ontario. In 2000, he was designated Fellow of the Chemical Institute of Canada. That same year, he was awarded the Medal of Research and Development from the Professional Engineers of Ontario. Hugo de Lasa received the Award in Industrial Practice in 2001 and the R. S. Jane Lecture Award in 2004, both from the Canadian Society for Chemical Engineering. In 2005, Hugo de Lasa was inducted as a Fellow of the Canadian Academy of Engineering. Hugo de Lasa received in 2005 an Honoris Causa degree from the Universidad Autonoma de Zacatecas, Mexico. In 2010, The American

Chemical Society published a special *Industrial and Engineering Chemistry Research Festschrift* issue in Hugo de Lasa's honor.



Enrique Salaices received his Ph.D. in Chemical Engineering in 2010 from The University of Western Ontario and his B.Sc. in Chemical Engineering in 1993 from the Universidad Autonoma de Zacatecas, Mexico. In 2006, he was awarded with a five-year Faculty of Graduates Studies, UWO—Mexican Government scholarship to pursue his Ph.D. studies in the area of catalytic steam gasification of biomass. Enrique Salaices is a Researcher at the Nuclear Energy Department of the Electric Power Research Institute, Mexico. Since this organization's inception in 1993, he has been collaborating in the development of safety analysis (thermohydraulics, corrosion, hydrogen injection, radiolytic gas accumulation, and detonation) and probabilistic risk assessment. This is being done for the evaluation of operational strategies in nuclear power plants and industrial facilities.



A. S. M. Jahirul Islam Mazumder is a Ph.D. candidate with an Alexander Graham Bell Canada Graduate Scholarship (NSERC-CGS) in the Department of Chemical and Biochemical Engineering at The University of Western Ontario. He is working on catalyst development and kinetic modeling for steam gasification of biomass under the supervision of Hugo de Lasa. In 2008, he obtained his M.E.Sc. from the same department. He developed a comprehensive model and performed multiobjective optimization of a liquid–solid circulating fluidized-bed system. This was done during his M.E.Sc. under the supervision of A. Ray and J. Zhu, for a continuous protein recovery. He completed his B.Sc. degree in chemical engineering from Bangladesh University of Engineering & Technology in 2005.



Rahima Akter Lucky received her Ph.D. degree in Chemical Engineering from the University of Western Ontario, Canada, in 2008. She had previously completed her B.Sc. (1997) and M.Sc. (1999) degrees, both in Chemical Engineering, from Bangladesh University of Engineering and Technology. Following her Ph.D., Dr. Lucky joined Chemical Reactor Engineering Centre at the University of Western Ontario as a postdoctoral fellow. Her research has been focused on synthesis and characterization of advanced nanomaterials using supercritical fluids. She is concentrating her efforts on advanced materials in a wide range of applications such as in advanced catalysts for biomass gasification and photovoltaics and nanocubes for hydrogen storage devices.

## ACKNOWLEDGMENT

We would gladly like to acknowledge the financial support of the Natural Sciences and Engineering Research Council of Canada (NSERC) who supported this research with a postgraduate scholarship awarded to J.M. and a PDF fellowship given to R.L. We are also thankful to CONACYT-Mexico who provided an external scholarship to E.S. to develop his Ph.D. research at the University of Western Ontario. We would also like to express our appreciation to Ms. Florencia de Lasa who provided valuable support with the diagrams as well as with the writing style of this manuscript.

## NOTATION

$daf$	dry ash free
DRM	dry reforming of methane reaction
$E_i$	activation energy in kJ/mol
ER	equivalence ratio as defined in eq 1
$j$	subscript to denote each component
K	Equilibrium reaction constant (-)
$k'_i$	kinetic constant lumping adsorption and intrinsic kinetic parameters
$k_i^k$	kinetic constant for component $i$ in mol/(g <sub>cat</sub> min)
$k_i^0$	pre-exponential factor
$k_{\text{DRM}}$	kinetic constant for the dry reforming of methane
$k_{\text{SR}}$	kinetic constant for the steam reforming of methane
$k_{\text{WGS}}$	kinetic constant for the water gas shift reaction
$K_i^A$	adsorption constant for component $i$ in 1/atm
$K_{\text{DRM}}$	equilibrium constant for the dry reforming of methane
$K_{\text{SR}}$	equilibrium constant for the steam reforming of methane
$K_{\text{WGS}}$	equilibrium constant for the water gas shift reaction
$m$	number of data points

$n$	number of chemical species
$p_i$	partial pressure of component $i$ in atm
$P_o$	total pressure in atm
$R$	universal gas constant
$r_i$	rate of reaction of component $i$ in mol/(g <sub>cat</sub> min)
$r_{\text{WGS}}$	water gas shift reaction rate
$r_{\text{SR}}$	steam reforming of methane reaction rate
$r_{\text{DRM}}$	dry reforming of methane reaction rate contribution
$R$	gas constant in atm cm <sup>3</sup> mol <sup>-1</sup> K <sup>-1</sup>
S/B	steam biomass ratio in kg/kg
SRM	steam reforming of methane reaction
T	Temperature (°K)
$y_i$	molar fraction of $i$ species
WGS	water gas shift reaction

## GREEK SYMBOLS

$\Delta H_{\text{ads}}^{\text{CO}_2}$	carbon dioxide heat of adsorption
$\sigma$	standard deviation
$\phi_i$	fugacity coefficient of $i$ species
$\Delta G^\circ$	standard Gibbs energy change of reaction (kJ/mole)
$\Delta H^\circ$	standard enthalpy change of reaction (kJ/mole)
$\nu_i$	stoichiometric coefficient of species "i"
$\nu$	sum of stoichiometric coefficients
$\nu_{\text{WGS},i}$	stoichiometric coefficient for the chemical species "i" involved in water gas shift reaction
$\nu_{\text{WGS},r}$	stoichiometric coefficient for the reference chemical species in water gas shift reaction (positive 1, based on H <sub>2</sub> )
$\nu_{\text{SR},i}$	stoichiometric coefficient for the chemical species "i" involved in steam reforming
$\nu_{\text{SR},r}$	stoichiometric coefficient for the reference chemical species in steam reforming (positive 1, based on CO formed)
$\nu_{\text{DR},i}$	stoichiometric coefficient for the chemical species "i" involved in dry reforming
$\nu_{\text{DR},r}$	stoichiometric coefficient for the reference chemical species in dry reforming (negative 1, based on CH <sub>4</sub> consumed)

## ACRONYMS

CREC	Chemical Reactor Engineering Centre
------	-------------------------------------

## REFERENCES

- (1) Balat, M. *Energy Sources, Part A* **2009**, *31*, 516.
- (2) Kuramoto, K.; Matsuoka, K.; Murakami, T.; Takagi, H.; Nanba, T.; Suzuki, Y.; Hosokai, S.; Hayashi, J.-i. *Ind. Eng. Chem. Res.* **2009**, *48*, 2851.
- (3) Demirbas, M. F. *Energy, Explor. Exploit.* **2005**, *23*, 215.
- (4) Chew, T. L.; Bhatia, S. *Bioresour. Technol.* **2008**, *99*, 7911.
- (5) Huber, G. W.; Iborra, S.; Corma, A. *Chem. Rev.* **2006**, *106*, 4044.
- (6) Torres, W.; Pansare, S. S.; Goodwin, J. G. *Evolution* **2007**, *49*, 407.
- (7) Khan, A.; Dejong, W.; Jansens, P.; Spliethoff, H. *Fuel Process. Technol.* **2009**, *90*, 21.
- (8) Belgiorno, V. *Waste Manage.* **2003**, *23*, 1.
- (9) Milne, A.; Evans, J.; Abatzoglou, N. NREL/TP-570-25357; National Renewable Energy Laboratories: Golden, CO, 1998.
- (10) Devi, L.; Ptasinska, K. J.; Janssena, F. J. J. G. *Biomass Bioenergy* **2003**, *24*, 125.
- (11) Abu El-Rub, Z.; Bramer, E.; Brem, G. *Ind. Eng. Chem. Res.* **2004**, *43*, 6911.

- (12) Boissonnet, G.; Bayle, J.; Seiler, J. M.; Chataing, T.; Rouge, S.; Bertrand, C. In *First European Hydrogen Energy Conference*; Grenoble, France, 2003.
- (13) Liao, C.; Wu, C.; Yan, Y. *Fuel Process. Technol.* **2007**, *88*, 149.
- (14) Dhepe, P. L.; Fukuoka, A. *ChemSusChem* **2008**, *1*, 969.
- (15) Dietenberger, M. a.; Anderson, M. *Ind. Eng. Chem. Res.* **2007**, *46*, 8863.
- (16) Digman, B.; Joo, S.; Kim, D.-s. *Environ. Prog. Sustainable Energy* **2009**, *28*, 47.
- (17) Xu, C.; Donald, J.; Byambajav, E.; Ohtsuka, Y. *Fuel* **2010**, *89*, 1784.
- (18) Leibold, H.; Hornung, A.; Seifert, H. *Powder Technol.* **2008**, *180*, 265.
- (19) Salaices, E.; Serrano, B.; de Lasa, H. *Ind. Eng. Chem. Res.* **2010**, *49*, 6834.
- (20) Sutton, D.; Kelleher, B.; Ross, J. R. H. *Fuel Process. Technol.* **2001**, *73*, 155.
- (21) Arauzo, J.; Radlein, D.; Piskorz, J.; Scott, D. S. *Ind. Eng. Chem. Res.* **1997**, *36*, 67.
- (22) Olivares, A.; Aznar, M. P.; Caballero, M. a; Gil, J.; Francés, E.; Corella, J. *Ind. Eng. Chem. Res.* **1997**, *36*, 5220.
- (23) Garcia, L.; Benedicto, A.; Romeo, E.; Salvador, M. L.; Arauzo, J.; Bilbao, R. *Energy Fuels* **2002**, *16*, 1222.
- (24) Garcia, L.; Salvador, M. L.; Arauzo, J.; Bilbao, R. *Energy Fuels* **1999**, *13*, 851.
- (25) Garcia, L.; Salvador, M. L.; Bilbao, R.; Arauzo, J. *Energy Fuels* **1998**, *12*, 139.
- (26) Arauzo, J.; Radlein, D.; Piskorz, J.; Scott, D. S. *Energy Fuels* **1994**, *8*, 1192.
- (27) Salaices, E. Ph.D. Dissertation; The University of Western Ontario, Canada, 2010.
- (28) Lu, Y.; Jin, H.; Guo, L.; Zhang, X.; Cao, C.; Guo, X. *Int. J. Hydrogen Energy* **2008**, *33*, 6066.
- (29) Hao, X. *Int. J. Hydrogen Energy* **2003**, *28*, 55.
- (30) Schmieder, H.; Abeln, J.; Boukis, N.; Dinjus, E.; Kruse, A.; Kluth, M.; Petrich, G.; Sadri, E.; Schacht, M. *J. Supercrit. Fluids* **2000**, *17*, 145.
- (31) Yanik, J.; Ebale, S.; Kruse, A.; Saglam, M.; Yüksel, M. *Int. J. Hydrogen Energy* **2008**, *33*, 4520.
- (32) Demirbas, A. *Energy Sources, Part B* **2007**, *2*, 227.
- (33) Briens, C.; Piskorz, J.; Berruti, F. *Int. J. Chem. React. Eng.* **2008**, *6*, 1.
- (34) Huang, H.-J.; Ramaswamy, S. *Appl. Biochem. Biotechnol.* **2009**, *154*, 193.
- (35) Roy, P. C.; Datta, A.; Chakraborty, N. *Renewable Energy* **2010**, *35*, 379.
- (36) Ni, M.; Leung, D.; Leung, M.; Sumathy, K. *Fuel Process. Technol.* **2006**, *87*, 461.
- (37) Rulkens, W. *Energy Fuels* **2008**, *22*, 9.
- (38) Frandsen, F. *J. Fuel* **2005**, *84*, 1277.
- (39) Leiva, C.; Gómez-Barea, A.; Vilches, L. F.; Ollero, P.; Vale, J.; Fernández-Pereira, C. *Energy Fuels* **2007**, *21*, 361.
- (40) Munir, S.; Daood, S. S.; Nimmo, W.; Cunliffe, A. M.; Gibbs, B. M. *Bioresour. Technol.* **2009**, *100*, 1413.
- (41) Chen, Y.; Luo, Y.-h.; Wu, W.-g.; Su, Y. *Energy Fuels* **2009**, *23*, 4659.
- (42) Kosstrin, H. In *Proceedings Specialists Workshop on Fast Pyrolysis of Biomass*; Copper Mountain, CO, 1980.
- (43) Han, J.; Kim, H. *Renewable Sustainable Energy Rev.* **2008**, *12*, 397.
- (44) Li, C.; Suzuki, K. *Renewable Sustainable Energy Rev.* **2009**, *13*, 594.
- (45) Borodulya, V. a.; Pal'chenok, G. I.; Rabinovich, O. S.; Vasilevich, S. V. *J. Eng. Phys. Thermophys.* **2007**, *80*, 322.
- (46) Mohan, D.; Pittman, C. U.; Steele, P. H. *Energy Fuels* **2006**, *20*, 848.
- (47) Antal, M. J.; Allen, S. G.; Schulman, D.; Xu, X.; Divilio, R. J. *Ind. Eng. Chem. Res.* **2000**, *39*, 4040.
- (48) Wei, L.; Xu, S.; Zhang, L.; Liu, C.; Zhu, H.; Liu, S. *Int. J. Hydrogen Energy* **2007**, *32*, 24.
- (49) Tomishige, K.; Asadullah, M.; Kunimori, K. *Catal. Today* **2004**, *89*, 389.
- (50) Franco, C.; Pinto, F.; Gulyurtlu, I.; Cabrita, I. *Fuel* **2003**, *82*, 835.
- (51) Ginsburg, J.; de Lasa, H. I. *Int. J. Chem. React. Eng.* **2005**, *3*, 1.
- (52) Aznar, M.; Caballero, M.; Sancho, J.; Frances, E. *Fuel Process. Technol.* **2006**, *87*, 409.
- (53) Kirubakaran, V.; Sivaramakrishnan, V.; Nalini, R.; Sekar, T.; Premalatha, M.; Subramanian, P. *Renewable Sustainable Energy Rev.* **2009**, *13*, 179.
- (54) McKendry, P. *Bioresour. Technol.* **2002**, *83*, 37.
- (55) Hrdlicka, J.; Feik, C.; Carpenter, D.; Pomeroy, M. NREL/TP-510-44557; National Renewable Energy Laboratories: Golden, CO, 2008.
- (56) Chaiwat, W.; Hasegawa, I.; Mae, K. *Ind. Eng. Chem. Res.* **2009**, *48*, 8934.
- (57) Elliot, D. In *In Proceedings ACS Symposium Series 376, Pyrolysis Oils From Biomass*; Denver, CO, 1988; p 55.
- (58) Barneto, A. G.; Carmona, J. A.; Conesa, J. a. *Energy Fuels* **2009**, *23*, 951.
- (59) Fushimi, C.; Katayama, S.; Tsutsumi, A. *J. Anal. Appl. Pyrolysis* **2009**, *86*, 82.
- (60) Hosoya, T.; Kawamoto, H.; Saka, S. *J. Wood Sci.* **2007**, *53*, 351.
- (61) Petrus, L.; Noordermeer, M. a. *Green Chem.* **2006**, *8*, 861.
- (62) Hosoya, T.; Kawamoto, H.; Saka, S. *J. Anal. Appl. Pyrolysis* **2007**, *80*, 118.
- (63) Lv, D.; Xu, M.; Liu, X.; Zhan, Z.; Li, Z.; Yao, H. *Fuel Process. Technol.* **2010**, *91*, 903.
- (64) Wu, H.; Yip, K.; Tian, F.; Xie, Z.; Li, C.-Z. *Ind. Eng. Chem. Res.* **2009**, *48*, 10431.
- (65) Banowetz, G. M.; Griffith, S. M.; El-Nashaar, H. M. *Energy Fuels* **2009**, *23*, 502.
- (66) Wang, L.; Weller, C.; Jones, D.; Hanna, M. *Biomass Bioenergy* **2008**, *32*, 573.
- (67) Skoulou, V.; Kantarelis, E.; Arvelakis, S.; Yang, W.; Zabaniotou, A. *Int. J. Hydrogen Energy* **2009**, *34*, 5666.
- (68) Raveendran, K.; Ganesh, A.; Khilart, K. C. *Fuel* **1995**, *74*, 1812.
- (69) Sinthaworn, S.; Nimityongskul, P. *Waste Manage.* **2009**, *29*, 1526.
- (70) Der Drift, A. van; Doorn, J.; van; Vermeulen, J. W. *Biomass Bioenergy* **2001**, *20*, 45.
- (71) Wang, L.; Hanna, M. A.; Weller, C. L.; Jones, D. D. *Energy Convers. Manage.* **2009**, *50*, 1704.
- (72) Hanaoka, T.; Inoue, S.; Uno, S.; Ogi, T.; Minowa, T. *Biomass Bioenergy* **2005**, *28*, 69.
- (73) Van Krevelen, D. W. *Coal—Typology—Physics—Chemistry—Constitution*, 3rd ed.; Elsevier: Amsterdam, The Netherlands, 1993.
- (74) Prins, M.; Ptasiński, K.; Janssen, F. *Energy* **2007**, *32*, 1248.
- (75) McKendry, P. *Bioresour. Technol.* **2002**, *83*, 55.
- (76) Zhou, Z.-q.; Ma, L.-l.; Yin, X.-l.; Wu, C.-z.; Huang, L.-c.; Wang, C. *Biotechnol. Adv.* **2009**, *27*, 612.
- (77) Maa, P.; Bailie, R. *Combust. Sci. Technol.* **1973**, *7*, 257.
- (78) Erlich, C.; Bjornbom, E.; Bolado, D.; Giner, M.; Fransson, T. *Fuel* **2006**, *85*, 1535.
- (79) Asadullah, M.; Zhang, S.; Min, Z.; Yimsiri, P.; Li, C.-Z. *Ind. Eng. Chem. Res.* **2009**, *48*, 9858.
- (80) Lange, J.-p. *Biofuel, Bioprod. Biorefin.* **2007**, *1*, 39.
- (81) Evans, R. J.; Milne, T. A. *Energy Fuels* **1987**, *1*, 123.
- (82) Fu, P.; Hu, S.; Sun, L.; Xiang, J.; Yang, T.; Zhang, A.; Zhang, J. *Bioresour. Technol.* **2009**, *100*, 4877.
- (83) Baker, E. G.; Mudge, L. K. *J. Anal. Appl. Pyrolysis* **1984**, *6*, 285.
- (84) Evans, R. J.; Milne, T. A.; Soltys, M. N. *J. Anal. Appl. Pyrolysis* **1986**, *9*, 207.
- (85) Zhang, J.; Toghiani, H.; Mohan, D.; Pittman, C. U.; Toghiani, R. K. *Energy Fuels* **2007**, *21*, 2373.
- (86) Yung, M. M.; Jablonski, W. S.; Magrini-Bair, K. A. *Energy Fuels* **2009**, *23*, 1874.

- (87) Goyal, H.; Seal, D.; Saxena, R. *Renewable Sustainable Energy Rev.* **2008**, *12*, 504.
- (88) Gordillo, G.; Annamalai, K.; Carlin, N. *Renewable Energy* **2009**, *34*, 2789.
- (89) Nagel, F. P.; Schildhauer, T. J.; McCaughey, N.; Biollaz, S. M. A. *Int. J. Hydrogen Energy* **2009**, *34*, 6826.
- (90) Sheth, P. N.; Babu, B. V. *Bioresour. Technol.* **2009**, *100*, 3127.
- (91) Bartels, M.; Lin, W.; Nijenhuis, J.; Kapteijn, F.; Vanommen, J. *Prog. Energy Combust. Sci.* **2008**, *34*, 633.
- (92) Visser, H. J. M.; Lith, S. C.; van; Kiel, J. H. A. *J. Energy Res. Technol.* **2008**, *130*, 1.
- (93) Osowski, S.; Neumann, J.; Fahnenkamp, H. *Chem. Eng. Technol.* **2005**, *28*, 596.
- (94) Corella, J.; Toledo, J. M.; Molina, G. *Ind. Eng. Chem. Res.* **2007**, *46*, 6831.
- (95) Tasaka, K.; Furusawa, T.; Tsutsumi, A. *Energy Fuels* **2007**, *21*, 590.
- (96) Pfeifer, C.; Puchner, B.; Hofbauer, H. *Chem. Eng. Sci.* **2009**, *64*, 5073.
- (97) Proll, T.; Rauch, R.; Aichernig, C.; Hofbauer, H. *Int. J. Chem. React. Eng.* **2007**, *5*, 1.
- (98) Osowski, S.; Fahnenkamp, H. *Ind. Crops Prod.* **2006**, *24*, 196.
- (99) Choudhary, V.; Banerjee, S.; Rajput, A. M. *J. Catal.* **2001**, *198*, 136.
- (100) Gassner, M.; Maréchal, F. *Energy* **2009**, *34*, 1744.
- (101) Wei, L.; Xu, S.; Liu, J.; Lu, C.; Liu, S.; Liu, C. *Energy Fuels* **2006**, *20*, 2266.
- (102) Warnecke, R. *Biomass Bioenergy* **2000**, *18*.
- (103) Demirbas, A. *Energy Sources* **2004**, *26*, 715.
- (104) Corella, J.; Toledo, J.-M.; Molina, G. *Int. J. Oil, Gas Coal Technol.* **2008**, *1*, 194.
- (105) Walawender, W.; Hoveland, D.; Fan, L. In *Fundamentals of thermochemical biomass conversion*; Elsevier: Amsterdam, The Netherlands, 1985; p 813.
- (106) Singh, S.; Walawender, W.; Fan, L.; Geyer, W. *Wood and fiber science*; Pergamon Press: New York, 1986; Vol. 6, pp 53.
- (107) Prasad, B. V. R. K.; Kuester, J. L. *Ind. Eng. Chem. Res.* **1988**, *27*, 304.
- (108) Herguido, J.; Corella, J.; Gonzalez-Saiz, J. *Ind. Eng. Chem. Res.* **1992**, *31*, 1274.
- (109) Mevissen, N.; Schulzke, T.; Unger, C. A.; Mac, S. *Environ. Prog. Sustainable Energy* **2009**, *28*, 347.
- (110) Narváez, I.; Orío, A.; Aznar, M. P.; Corella, J. *Ind. Eng. Chem. Res.* **1996**, *35*, 2110.
- (111) Lv, P.; Chang, J.; Wang, T.; Wu, C.; Tsubaki, N. *Energy Fuels* **2004**, *18*, 1865.
- (112) Garcia-Ibanez, P.; Cabanillas, A.; Sanchez, J. *Biomass Bioenergy* **2004**, *27*, 183.
- (113) Courson, C.; Makaga, E.; Petit, C.; Kiennemann, A. *Catal. Today* **2000**, *63*, 427.
- (114) Zhou, J.; Masutani, S. M.; Ishimura, D. M.; Turn, S. Q.; Kinoshita, C. M. *Ind. Eng. Chem. Res.* **2000**, *39*, 626.
- (115) Palancar, M. C.; Serrano, M.; Aragón, J. M. *Powder Technol.* **2009**, *194*, 42.
- (116) Hanping, C.; Bin, L.; Haiping, Y.; Guolai, Y.; Shihong, Z. *Energy Fuels* **2008**, *22*, 3493.
- (117) Skoulou, V.; Swiderski, A.; Yang, W.; Zabaniotou, A. *Bioresour. Technol.* **2009**, *100*, 2444.
- (118) Luo, S.; Xiao, B.; Hu, Z.; Liu, S.; Guo, X.; He, M. *Int. J. Hydrogen Energy* **2009**, *34*, 2191.
- (119) Gao, N.; Li, A.; Quan, C. *Bioresour. Technol.* **2009**, *100*, 4271.
- (120) Mahishi, M.; Goswami, D. *Int. J. Hydrogen Energy* **2007**, *32*, 3831.
- (121) Wolfesberger, U.; Aigner, I.; Hofbauer, H. *Environ. Prog. Sustainable Energy* **2009**, *28*, 372.
- (122) Fagbemi, L.; Khezami, L.; Capart, R. *Appl. Energy* **2001**, *69*, 293.
- (123) Zhao, Y.; Sun, S.; Tian, H.; Qian, J.; Su, F.; Ling, F. *Bioresour. Technol.* **2009**, *100*, 6040.
- (124) Knight, R. *Biomass Bioenergy* **2000**, *18*, 67.
- (125) Wang, W.; Ye, Z.; Padban, N.; Olofsson, G.; Bjerle, I. In *Proceedings First World Conference on Biomass for Energy and Industry*; Kyritsis, S., Beenackers, A., Helm, P., Grassi, A., Chiaramonti, D., Eds.; Seville, Spain, 2000; p 1698.
- (126) Li, X. T.; Grace, J. R.; Watkinson, A. P.; Lim, C. J.; Ergudenler, A. *Fuel* **2001**, *80*, 195.
- (127) Li, X. T.; Grace, J. R.; Lim, C. J.; Watkinson, A. P.; Chen, H. P.; Kim, J. R. *Biomass Bioenergy* **2004**, *26*, 171.
- (128) Gil, J.; Corella, J.; Aznar, M. P.; Caballero, M. A. *Biomass Bioenergy* **1999**, *17*, 389.
- (129) Fiaschi, D.; Michelini, M. *Biomass Bioenergy* **2001**, *21*, 121.
- (130) Mathieu, P.; Dubuisson, R. *Energy Convers. Manage.* **2002**, *43*, 1291.
- (131) Zhang, R.; Brown, R.; Suby, A.; Cummer, K. *Energy Convers. Manage.* **2004**, *45*, 995.
- (132) Rapagna, S.; Provendier, H.; Petit, C.; Kiennemann, A.; Foscolo, P. *Biomass Bioenergy* **2002**, *22*, 377.
- (133) Rapagna, S.; Latif, A. *Biomass Bioenergy* **1997**, *12*, 281.
- (134) García, X.; Alarcon, N.; Gordon, A. *Fuel Process. Technol.* **1999**, *58*, 83.
- (135) Minowa, T.; Inoue, S. *Renewable Energy* **1999**, *16*, 1114.
- (136) Schuster, G.; Loffler, G.; Weigl, K.; Hofbauer, H. *Bioresour. Technol.* **2001**, *77*, 71.
- (137) Coll, R. *Fuel Process. Technol.* **2001**, *74*, 19.
- (138) Kinoshita, C. M.; Wang, Y.; Zhou, J. *J. Anal. Appl. Pyrolysis* **1994**, *29*, 169.
- (139) Corella, J.; Aznar, M.-P.; Gil, J.; Caballero, M. A. *Energy Fuels* **1999**, *13*, 1122.
- (140) Banowetz, G. M.; Griffith, S. M.; El-Nashaar, H. M. *Energy Fuels* **2009**, *23*, 502.
- (141) Asadullah, M.; Fujimoto, K.; Tomishige, K. *Ind. Eng. Chem. Res.* **2001**, *40*, 5894.
- (142) Mudge, L. K.; Baker, E. G.; Mitchell, D. H.; Brown, M. D. *J. Solar Energy Eng.* **1985**, *107*, 88.
- (143) Baker, E. G.; Mudge, L. K.; Brown, M. D. *Ind. Eng. Chem. (Anal. Ed.)* **1987**, *26*, 1335.
- (144) Liu, H.; Chen, T.; Zhang, X.; Li, J.; Chang, D.; Song, L. *Chin. J. Catal.* **2010**, *31*, 409.
- (145) Nishikawa, J.; Nakamura, K.; Asadullah, M.; Miyazawa, T.; Kunimori, K.; Tomishige, K. *Catal. Today* **2008**, *131*, 146.
- (146) Caballero, M. a.; Corella, J.; Aznar, M.-P.; Gil, J. *Ind. Eng. Chem. Res.* **2000**, *39*, 1143.
- (147) Caballero, M. a.; Aznar, M. P.; Gil, J.; Martín, J. a.; Francés, E.; Corella, J. *Ind. Eng. Chem. Res.* **1997**, *36*, 5227.
- (148) Aznar, M. P.; Caballero, M. a.; Gil, J.; Martín, J. a.; Corella, J. *Ind. Eng. Chem. Res.* **1998**, *37*, 2668.
- (149) Corella, J.; Orío, A.; Aznar, P. *Ind. Eng. Chem. Res.* **1998**, *37*, 4617.
- (150) Kinoshita, C. M.; Wang, Y.; Zhou, J. *Ind. Eng. Chem. Res.* **1995**, *34*, 2949.
- (151) Asadullah, M.; Tomishige, K.; Fujimoto, K. *Catal. Commun.* **2001**, *2*, 63.
- (152) Florin, N.; Harris, A. *Chem. Eng. Sci.* **2008**, *63*, 287.
- (153) Dalai, A. K.; Sasaoka, E.; Hikita, H.; Ferdous, D. *Energy Fuels* **2003**, *17*, 1456.
- (154) Hu, G.; Xu, S.; Li, S.; Xiao, C.; Liu, S. *Fuel Process. Technol.* **2006**, *87*, 375.
- (155) Devi, L.; Ptasinska, K. J.; Janssena, F. J. J. G.; Paasenb, S. V. B. V.; Bergmanb, P. C. A.; Kiel, J. H. A. *Renewable Energy* **2005**, *30*, 565.
- (156) Xu, G.; Murakami, T.; Suda, T.; Kusama, S.; Fujimori, T. *Ind. Eng. Chem. Res.* **2005**, *44*, 5864.
- (157) Quyn, D. M.; Wu, H.; Li, C.-Z. *Fuel* **2002**, *81*, 143.
- (158) Quyn, D. M.; Wu, H.; Bhattacharya, S. P.; Li, C.-Z. *Fuel* **2002**, *81*, 151.
- (159) Wu, H.; Quyn, D. M.; Li, C.-Z. *Fuel* **2002**, *81*, 1033.
- (160) Lee, S. W.; Nam, S. S.; Kim, S. B.; Lee, K. W.; Choi, C. S. *Korean J. Chem. Eng.* **2000**, *17*, 174.

- (161) Simell, P. A.; Leppalahti, J. K.; Bredenberg, J. B. *Fuel* **1992**, *71*, 211.
- (162) Juutilainen, S.; Simell, P.; Krause, A. *Appl. Catal., B* **2006**, *62*, 86.
- (163) Rostrup-Nielsen, J. R.; Hansen, J.-H. B. **1993**, *144*, 38.
- (164) Elliott, D. C.; Baker, E. G.; Butner, R. S.; Sealock, L. J. *J. Solar Energy Eng.* **1993**, *115*, 52.
- (165) Aznar, M. P.; Corella, J.; Delgado, J.; Lahoz, J. *Ind. Eng. Chem. Res.* **1993**, *32*, 1.
- (166) Trimm, D. L. *Catal. Today* **1997**, *37*, 233.
- (167) Bartholomew, C. H.; Sorensen, W. L. *J. Catal.* **1983**, *81*, 131.
- (168) Bartholomew, C. H.; Weatherbee, G. D.; Jarvi, G. A. *Chem. Eng. Commun.* **1980**, *5*, 125.
- (169) Bangala, D. N.; Abatzoglou, N.; Chornet, E. *AIChE J.* **1998**, *44*, 927.
- (170) Rostrup-Nielsen, J. R. *Catal. Today* **1997**, *37*, 225.
- (171) Dibbern, H. C.; Olesen, P.; Rostrup-Nielsen, J. R.; Tottrup, P. B.; Udengaard, N. R. *Hydrocarbon Process.* **1986**, *65*, 71.
- (172) Tomishige, K.; Asadullah, M.; Kunimori, K. *Catal. Surv. Asia* **2003**, *7*, 219.
- (173) Struis, R. P. W. J.; Schildhauer, T. J.; Czekaj, I.; Janousch, M.; Biollaz, S. M. a.; Ludwig, C. *Appl. Catal., A* **2009**, *362*, 121.
- (174) Sato, K.; Fujimoto, K. *Catal. Commun.* **2007**, *8*, 1697.
- (175) Wang, S.; Lu, G. Q. *Appl. Catal., A* **1998**, *169*, 271.
- (176) Wang, S.; Lu, G. Q. M. *Appl. Catal., B* **1998**, *16*, 269.
- (177) Mark, M. F.; Maier, W. F. *J. Catal.* **1996**, *164*, 122.
- (178) Gadalla, A. M.; Bower, B. *Chem. Eng. Sci.* **1988**, *43*, 3049.
- (179) Higman, C.; van der Burgt, M. *Gasification*, 2nd ed.; Gulf Professional Publisher/Elsevier Science: Amsterdam, Boston, 2008.
- (180) Aktaş, S.; Karakaya, M.; Avci, A. K. *Int. J. Hydrogen Energy* **2009**, *34*, 1752.
- (181) Baratieri, M.; Baggio, P.; Fiori, L.; Grigiante, M. *Bioresour. Technol.* **2008**, *99*, 7063.
- (182) Altafini, C. R.; Mirandola, A. In *Proceedings Florence World Energy Research Symposium—FLOWERS'97*; Florence, Italy, 1997; p 419.
- (183) Ruggiero, M.; Manfrida, G. *Renewable Energy* **1999**, *16*, 1106.
- (184) Rapagna, S.; Jand, N.; KENNEMANN, A.; Foscolo, P. U. *Biomass Bioenergy* **2000**, *19*, 187.
- (185) Boissonnet, G.; Seiler, J. M.; Chataing, T.; Claudet, G.; Brothier, M.; Bertrand, C. In *Expert Meeting*; Strasbourg, France, 2002.
- (186) Kersten, S. R. A.; Prins, W.; Van Der Drift, A.; Van Swaaij, W. P. M. In *12th European Conference on Biomass for Energy, Industry and Climate Protection*; Amsterdam, The Netherlands, 2002.
- (187) Jand, N.; Brandani, V.; Foscolo, P. U. *Ind. Eng. Chem. Res.* **2006**, *45*, 834.
- (188) Melgar, A.; Perez, J.; Laget, H.; Horillo, A. *Energy Convers. Manage.* **2007**, *48*, 59.
- (189) Srinivas, T.; Gupta, a. V. S. S. K. S.; Reddy, B. V. J. *Energy Resour. Technol.* **2009**, *131*, 031801.
- (190) Smith, J. M.; Van Ness, H. C.; Abbott, M. M. *Introduction to Chemical Engineering Thermodynamics*, 5th ed.; The McGraw-Hill Companies, Inc.: 1996.
- (191) de Lasa, H. I. USA Patent 5,102,628 1992.
- (192) Ptasinski, K. J. *Biofuel, Bioprod. Biorefin.* **2008**, *2*, 239.
- (193) Toonissen, R.; Woudstra, N.; Verkooijen, A. H. M. *Int. J. Hydrogen Energy* **2008**, *33*, 4074.
- (194) Paviet, F.; Chazarenc, F.; Tazerout, M. *Int. J. Chem. React. Eng.* **2009**, *7*, 1.
- (195) Baggio, P.; Baratieri, M.; Fiori, L.; Grigiante, M.; Avi, D.; Tosi, P. *Energy Convers. Manage.* **2009**, *50*, 1426.
- (196) Dupont, C.; Boissonnet, G.; Seiler, J.; Gauthier, P.; Schweich, D. *Fuel* **2007**, *86*, 32.
- (197) Zanzi, R. Ph.D. Thesis, Royal Institute of Technology, Stockholm, Sweden, 2001.
- (198) Buekens, A. G.; Schoeters, J. G. *Modelling of Biomass Gasification: Fundamentals of Thermochemical Biomass Conversion*; Elsevier: London, 1982.
- (199) Moghtaderi, B. *Fuel* **2007**, *86*, 2422.
- (200) Haryanto, A.; Fernando, S. D.; Pordesimo, L. O.; Adhikari, S. *Biomass Bioenergy* **2009**, *33*, 882.
- (201) Wang, X.; Li, S.; Wang, H.; Liu, B.; Ma, X. *Energy Fuels* **2008**, *22*, 4285.
- (202) Pyle, D. L.; Zaror, C. A. *Chem. Eng. Sci.* **1985**, *39*, 147.
- (203) Bryden, K. M.; Ragland, K. W.; Rutland, C. J. **2002**, *22*, 41.
- (204) Simmons, G. M.; Gentry, M. J. *Anal. Appl. Pyrolysis* **1986**, *10*, 117.
- (205) Peters, B.; Bruch, C. *J. Anal. Appl. Pyrolysis* **2003**, *70*, 1.
- (206) Golfier, F.; Mermoud, F.; Salvador, S.; Dirion, J. L.; Van De Steene, L. In *2nd world conference on biomass for energy, industry and climate protection*; Rome, Italy, 2004.
- (207) Raman, P.; Walawender, W. P.; Fan, L. T.; Chang, C. C. *Ind. Eng. Chem. Process Dev.* **1981**, *20*, 686.
- (208) Di Blasi, C. *Chem. Eng. Sci.* **2000**, *55*, 2931.
- (209) Matsui, I.; Kunii, D.; Furusawa, T. *J. Chem. Eng. Jpn.* **1985**, *18*, 105.
- (210) Koufopanos, C. A.; Papayannakos, N. *Can. J. Chem. Eng.* **1991**, *69*, 907.
- (211) Lv, P.; Chang, J.; Wang, T.; Wu, C.; Tsubaki, N. *Energy Fuels* **2004**, *18*, 1865.
- (212) Radmanesh, R.; Chaouki, J.; Guy, C. *AIChE J.* **2006**, *52*, 4258.
- (213) Corella, J.; Sanz, A. *Fuel Process. Technol.* **2005**, *86*, 1021.
- (214) Kilpinen, P.; Hupa, M.; Leepalahti, J. *Nitrogen Chemistry at Gasification ± A Thermodynamic Analysis*; 1991.
- (215) Salaices, E.; Serrano, B.; de Lasa, H. *AIChE J.* **2011** in press.